PERFORMANCE ANALYSIS OF AN EARTH WATER HEAT EXCHANGER IN SHARJAH

by

Hanin Atwany

A Thesis presented to the Faculty of the
American University of Sharjah
College of Engineering
In Partial Fulfillment
of the Requirements
for the Degree of

Master of Science in
Mechanical Engineering

Sharjah, United Arab Emirates

November 2019

Approval Signatures

We, the undersigned, approve the Master's Thesis of Hanin Atwany

Thesis Title: Performance Analysis of An Earth Water Heat Exchanger in Sharjah.

Signature	**Date of Signature** (dd/mm/yyyy)
_____	_____
Dr. Mohammad Omar Hamdan Associate Professor, Department of Mechanical Engineering Thesis Advisor	
_____	_____
Dr. Bassam Abu-Nabah Associate Professor, Department of Mechanical Engineering Thesis Co-Advisor	
_____	_____
Dr. Mohamed Abdelgawad Associate Professor, Department of Mechanical Engineering Thesis Committee Member	
_____	_____
Dr. Mousa Attom Professor, Department of Civil Engineering Thesis Committee Member	
_____	_____
Dr. Mamoun Abdel-Hafez Head, Department of Mechanical Engineering	
_____	_____
Dr. Lotfi Romdhane Associate Dean for Graduate Affairs and Research College of Engineering	
_____	_____
Dr. Naif Darwish Acting dean, College of Engineering	
_____	_____
Dr. Mohamed El-Tarhuni Vice Provost for Graduate Studies	

Acknowledgement

My immense gratitude extends towards my advisor, mentor and guide Dr. Mohammad Hamdan, whose unlimited support lead to the completion of this work. I express my sincere appreciation to Dr. Bassam Abu-Nabah, for Co-advising this work.

I would also like to thank the thesis committee members, Dr. Mousa Attom and Dr. Mohamed Abdelgawad, for their valuable feedback and recommendations. My very special gratitude goes to the professors who taught me during my studies, Dr. Maen Alkhader, Dr. Wael Abuzaid, Dr. Mehmet Orhan, Dr. Mohamed Abdelgawad and Dr. Mohammad Hamdan. I am also grateful to the faculty that I worked with as a teaching assistant, Dr. Mehmet Kanoglu for believing in my capabilities, engineer Wasim Almasri and engineer Ali Wadi for their support. A special thanks to my unique friend Anfal Al Abdulla for making my masters journey remarkable.

Words can't serve my family right for their unparalleled love, compassion and support. I am forever indebted to my amazing parents who've always been by my side, my admirable sisters for believing in me and my adorable brothers for bringing joy to my life.

Last but not least, I am quite grateful to the American University of Sharjah, in particular the Mechanical Engineering department, for sponsoring my studies by granting me a teaching assistantship and funding my thesis project.

Dedication

To my forever supportive, encouraging and caring father,
and to my life-coach, loving mother,
both whom I owe all of my success…

Abstract

The growing global demand for energy is amplifying the need for the development of sustainable and energy efficient systems. In the Arabian Gulf, cooling load represents about 70% of the overall energy consumed during the peak summer season. While geothermal cooling has been identified as an effective method for reducing the cooling load, the utilization of Earth Water Heat Exchanges (EWHE) has not been given much attention in the Gulf region. The inadequate research and data available on EWHE technology has hindered its adoption for practical use during structural development and building construction in the United Arab Emirates. In order to bridge this gap, this study demonstrates a comprehensive analysis of the performance of the EWHE through evaluating three critical factors: soil properties, vertical ground temperature distribution, and the EWHE design parameters. The properties of soil are being evaluated through lab testing of soil samples. Vertical ground temperature distribution data is collected from two boreholes located in different locations over the course of seven months. A setup mimicking the performance of an EWHE has been built to collect real time data over several planned test runs. Based on the findings of the current experiments and data, a three-dimensional numerical simulation model has been developed using ANSYS Fluent Release 19.1 to investigate the performance of a horizontal EWHE. The experimental study verified the presence of a geothermal cooling potential in the United Arab Emirates. At a flow rate of 0.15 kg/s and water inlet temperature of 340 K, water outlet temperature was lower by 30 K. The numerical analysis indicated the possibility of further enhancing the rate of heat exchanged through imbedding the heat exchanger in a backfill material of higher soil thermal conductivity. Soil properties and temperature data collected, present a valuable input for future geothermal research in the region.

Keywords: ***Heat exchanger, Soil properties, Temperature distribution, Geothermal cooling, EWHE effectiveness.***

Table of Contents

List of Figures

List of Tables

List of Abbreviations

ASHP	Air Source Heat Pump
CFD	Computational Fluid Dynamics
COP	Coefficient of Performance
EAHE	Earth Air Heat Exchanger
EATHE	Earth Air Tunnel Heat Exchanger
EDS	Energy Dispersive Spectroscopy
EUT	Earth's Undisturbed Temperature
EWHE	Earth Water Heat Exchanger
GCHP	Ground Coupled Heat Pump
GHE	Ground Heat Exchanger
GSHP	Ground Source Heat Pump
HGCHP	Hybrid Ground Coupled Heat Pump
HGHE	Horizontal Ground Heat Exchanger
PV	Photovoltaic
SAHD	Solar Air Heating Duct
SEM	Scanning Electron Microscopy

Chapter 1. Introduction

In this chapter, a short introduction is provided about the use of earth water heat exchangers and studies investigating their performance. Then, we present the problem investigated in this study as well as the thesis contribution. Finally, a general organization of the thesis is presented.

1.1. Overview

Science is currently devoted to discovering technologies that are renewable, sustainable and clean. All of which are features exhibited by geothermal air-conditioning [1]. Geothermal heating or cooling refers to the employment of the stable earth temperatures to cool a building during summer season or heat it during the winter season [2].The Earth's massive thermal capacitance provides a passive mean of heating and cooling [3]. The energy saved maybe estimated based on the difference between the outside air and the ground temperature [4]. The introduction of geothermal heating and cooling is dated back to 1912 but was made feasible through the introduction of plastic pipes in the 1970s. It was suggested that EWHE would reduce peak demand and fossil fuel usage, thus reducing carbon emissions [5]. Despite the widely proven advantages of geothermal cooling, there are very few studies tackling its utilization in the Middle East [6]. That can be vindicated by the lack of data related to soil properties and vertical ground temperature distribution in the region. While there are different configurations of ground heat exchangers, a commonly used setup is the closed loop horizontal heat exchanger shown in Figure 1.1a. It consists of an array of pipes connected in series or parallel and buried at 1 to 2 meters beneath ground surface with a heat carrier medium flowing through, typically air or water. Figure 1.1 shows three commonly used configurations, with the horizontal pipe being widely adopted due to the ease of its low installation cost [7]. The key aim of altering the geometry is to maximize the contact surface area thus increasing the rate of heat transfer [8]. However, optimizing the system performance should take the economic factor into consideration. Thus, a configuration such as vertical slinky loop shown in Figure 1.1c was proposed in which the surface area is maximized without the need to occupy a large space [9]. In addition to studying the performance of numerous geometries, researchers investigated the effect of different fluids mainly air and water. In general, water heat exchangers are

preferable as they are easier to install given the smaller a diameter and less prone to water condensate in comparison to earth-air heat exchangers [10]. Overall, geothermal cooling can contribute to meeting the goal of net zero energy buildings by reducing the cooling loads which present the majority of the demand in the Middle East region [11].

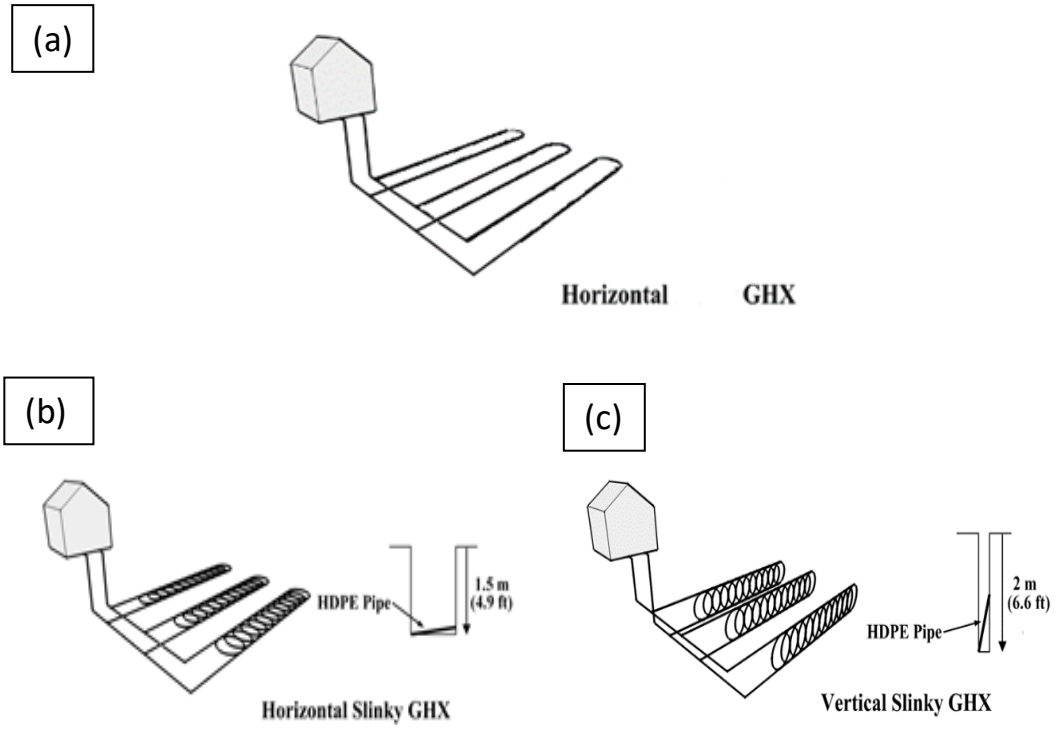

Figure 1.1: Earth water heat exchanger configurations [12].

This work provides a comprehensive literature review where related previous studies are discussed, followed by the methodology section on which details are provided on the experimental setup and all the methods used and finally concluded with some results, observations and future work.

1.2. Thesis Objectives

In consistence with the sustainable development goals to reduce consumption and utilize renewable resources, an increased interest in geothermal heat exchangers arises [13].

The rapid surge in energy demand driven by the increase in population is currently a universal concern. Several solutions have been proposed to approach this issue, some involving action on the demand side others on the supply side [14].

This study focuses on studying the performance of the earth-water heat exchangers within the United Arab Emirates. Through collecting critical data that is not available in databases including vertical ground temperature distribution, soil properties and composition. Followed by employing Numerical models to investigate various scenarios. The objective of this work is to develop an understanding of the performance of an earth heat exchanger for cooling and its contribution to load reduction in the United Arab Emirates.

1.3. Research Contribution

The goal of this work was to investigate the performance of an EWHE in the United Arab Emirates based on data collected from the project site. The analysis was performed to study the effect of various parameters and to optimize the performance in this region. Accordingly, the following objectives were achieved:

1. Evaluating the performance of horizontal ground loop Heat Exchanger by building a setup, consisting of 300 m long pipe buried at 2.5 m depth within the campus.
2. Collecting vertical ground temperature measurements in two different locations up to 10 meters depth over a period of one year.
3. Evaluating the thermal properties of soil at different water contents, compaction levels and particle distribution experimentally.
4. Utilizing Numerical methods (ANSYS FLUENT) in studying the performance of an Earth Water Heat Exchanger to maximize the rate of heat exchange.

1.4. Thesis Organization

The rest of the thesis is organized as follows: Chapter 2 provides background and literature review about geothermal cooling technology and models developed studying its performance. Moreover, work related to this research is discussed. The Methodology is discussed in Chapter 3 along with the implementation of the proposed setup of the trench and the boreholes. Chapter 4 presents the results obtained experimentally and numerically. Finally, Chapter 5 concludes the thesis and outlines the future work.

Chapter 2. Background and Literature Review

Utilizing the Earth capacitance for heating and cooling efficiently depends mainly on the system design. In general, there are two types of ground heat exchangers, closed and open loop systems. Where the fluid circulates in the closed but is drained after use in an open system. Closed systems are commonly used as they don't require a water source and a less prominent to collection of debris. Regardless of the type chosen, pipes maybe laid in vertical or horizontal configuration. Typical horizontal arrangements include series, parallel, trench and slinky [15]. For vertical type HEs, U-tube pipes and concentric or coaxial are commonly adopted designs. The performance of each is most accurately observed through experimental setups which provide reliable and concrete data. However, due to high costs, 1-D mathematical models that mimic the performance of a HE, were proposed earlier followed by 2-D and 3-D Numerical analysis in the recent years. Those models facilitate the understanding of a system performance given they are provided with valid input. Thus, validation of numerical results against experimental is necessary.

2.1. Experimental Studies

Performance of a ground heat exchanger is a function of geometrical characteristics, ground and pipe thermal characteristics, and ground temperature distribution. Reliability of Numerical simulations depends on their agreement with experimental results. Through matching numerical input parameters with experimental condition, results of both are expected to align in the presence of a valid model.

Hwang et al. [16] reported the cooling performance of a GSHP installed in a school building in Korea. The ground heat exchanger was a vertical closed loop with 24 boreholes that are 175 m deep. The overall system performance was evaluated based on the heat exchanger inlet/outlet temperatures, system cooling capacity and the input power. It was found that the average COP of the system was 5.9 which 74% higher than that of an ASHP system. This was attributed to the lower condensing temperature which indicates a lower power consumption by the compressor [16]. Sharqawy et al. [17] evaluated the thermal properties of soil including soil thermal conductivity, diffusivity and soil resistance using an in situ thermal response test. A setup of an 80 m deep vertical geothermal heat exchanger at the King Fahd University of Petroleum and

Minerals, Saudi Arabia was used to conduct the test. The change in the inlet and outlet temperature of the circulating water along with the line source theory were used to evaluate the soil thermal properties. The soil thermal conductivity, soil resistance and soil diffusivity were found to be 2.154 W/m.K, 0.315 m.K/W and 6.252×10^{6} m^2/s respectively [17]. Pulat et al. [18] investigated the performance of a horizontal ground heat exchanger buried at 2 m depth operating in the heating mode in Bursa, Turkey. The influence of GHE outlet water temperature and ambient air temperature in the southern Marmara region were taken into consideration. The study proved that GSP are the most effective method of heating in comparison to natural gas, LPG, fuel oil and electric resistance in terms of unit energy costs. A COP of 2.52 was obtained for the entire system and 4.25 for the HPU. Thus, it can be concluded that adoption of geothermal heating systems is feasible in regions as Bursa [18].

Bakirci et al. [19] prepared a setup of a vertical ground heat exchanger in Erzurum, Turkey operating in the heating mode. The hourly water outlet temperature was recorded from October to May and was used to calculate the system COP. It was deduced that average system COP was 2.9 which is relatively low, this was attributed to the design of the system [19]. Miyara et al. [20] studied the performance of 3 types of heat exchangers. Double tube, U- tube and multi tube with water as the heat transport medium. Thermocouples were placed along the length of the tubes to identify the ground temperature distribution and understand the effect of tube to tube interference. It was concluded that double U-tube results in the highest rate of heat exchange followed by the multi tube and the U tube. Furthermore, an increase in water flow rate was associated with an increase in the rate of heat exchanged for both multi and double but not U- tubes [20]. Florides et al. [21] reported ground temperature distribution in Cyprus over a period of a year to aid in assessing the performance of GCHP. The undisturbed ground temperature was observed at 7-8 meters depth and ranged between 18 to 23°C. A borehole installed in Athalassa with depth of 50 m was used to study the potential of heating and cooling using GCHPs. A significant decrease in energy consumption is predicted and vertical heat exchangers are assumed to provide a better performance in comparison to horizontal based on the temperature distribution obtained [21]. Karabacak et al. [22] analysed the cooling performance of a GSHP located in Denizli, Turkey. Vertical U-type pipe of 225 m in length and 110 m in depth was drilled. Thermocouples were placed for measuring ground temperature and soil samples for

testing were collected. The soil thermal conductivity was found to range between 0.55 and 2.242 W/m.K depending on the depth. The COP of the system which varied between 2.1 and 3.1 was found to be positively affected by wind speed but negatively by increase in solar radiation. Overall, ground heat exchangers present an economical alternative to air source heat exchangers given the high costs of electricity [22]. N. Hazami et al. [23] studied the possibility of utilizing Ground source heat pump for cooling in a hot climate region like Tunisia. The study consisted of two parts, the first part involved a parametric study of the parameters influencing a horizontal ground heat exchanger buried at 0.6 and 1 m depth. In the second part an experimental setup of a ground source cooling system was constructed. It was concluded that the ground temperature was nearly constant below 1 m depth and that there exists a non-linear positive relation between the rate of heat exchanged and the heat exchanger length. Overall, the ground source cooling proved to be a promising method of reducing the cooling demand in Tunisia [23]. Flaga-Maryanczyk et al. [24] recorded measurements of a ground source heat exchanger operating at a cold climate in Poland over a period of one year. The parallel horizontal ground heat exchanger was buried at a depth of 1.5 m and was used as a passive house ventilation system. For the given case, the ground heat exchanger was capable of providing 24% of the total heating load in February with an ambient air temperature of 266 K. Overall, the system utilized the ground thermal inertia overcoming the fluctuations in the outside air temperatures [24]. Vaz et al. [25] investigated the thermal potential of an EAHE experimentally by placing a setup in Brazil. An understanding of the ground transient thermal behavior was developed which aided in the findings of the best employment time. A total of three ducts were involved in the study buried at different depths ranging from 0.5 m to 1.6 m. The results indicated a higher ground potential for heating in comparison to cooling [25]. Cullin et al. [26] validated simulation in simulation-based design tool and ASHRAE handbook method for ground heat exchanger design 2011 using experimental data over 6 years of operation. The six vertical U-tube heat exchangers of 50 m depth were installed in Valencia, Spain. It was found that the predicted length of heat exchanger required using the simulation tool was within 5% of the actual in contrast to that predicted using ASHRAE Handbook design method which over predicted the length required by a factor of 2 [26]. Luo et al. [27] evaluated the performance of a GSHP connected to a vertical heat exchanger in the heating and cooling mode over a period of 4 years. The

system was connected to building in Germany with a cooling load higher than the heating load. Thus, results indicated a decreasing performance in the cooling mode in contrast to the heating mode due to the uneven distribution of the loads. A temperature difference of 3°C and 1.5°C was obtained between the inlet and outlet fluid of the heat exchanger in the heating mode and cooling mode respectively [27]. Serageldin et al. [28] studied the performance of a horizontal earth air heat exchanger buried at 2 m depth in the Egyptian climate conditions comprehensively. A system setup was used to evaluate air cooling and heating potential. A model was used to perform a parametric study evaluating the influence of pipe diameter, pipe material, pipe spacing and pipe length on the overall performance. The model was validated against experimental results and showed good agreement. The highlighted findings include a decrease in the air temperature in response to increasing the pipe diameter. A counter effect was observed on air temperature when increasing the pipe length. A change in temperature of 3°C was achieved in a pipe length of 5.5 m [28]. Sivasakthivel et al. [29] evaluated the heat rate and effectiveness of a GSHP operating in the heating and cooling mode in India. A U-tube heat exchanger 8.5 m in length with water as the working fluid was monitored over 8 hours of operation in 5 trials for each mode over a period of a year. In general, the performance was found to degrade with time with an increase in thermal resistance of the ground. A higher rate of heat exchange was observed for heating in comparison to cooling [29]. Sivasakthivel et al. [30] evaluated the thermal performance of single and double U-tube heat exchangers at various operating conditions. Operating hours were varied between 8, 16, 30 and 50 hours. In the case of short-term operation, the double U-tube heat exchanger exhibited 12% more heat exchange in comparison to the set level. While the single U-tube heat exchanger was capable of meeting only 80% of the set level. Furthermore, the average effectiveness of single U-tube was 26% and 30% less than that of the double U-tube in the case of heating and cooling respectively [30]. Zhai et al. [31] designed a mini type GSHP coupled to 9 vertical U-type HEs to cover the heating and cooling load of a 180 m^2 meeting room. The experimental setup was built in China and operated automatically. The soil temperature was recorded over a period of one year and no variation in temperature was observed. That was attributed to the balanced load which maintained the thermal balance in earth energy. The COP was found to be 3 and 3.2 in the heating and cooling mode respectively [31].

Table 2.1: Experimental Studies.

Configuration	Mode	Fluid	Location	Outcome	Reference
Vertical GHE	Cooling	Water	Korea	COP pf GSHP is 74% higher than that of ASHP	[16]
Vertical GHE	Cooling	Water	KSA	Ground resistance in KSA of 0.315 mK/W	[17]
Horizontal GHE	Heating	Water	Turkey	Geothermal heating is feasible in Bursa, Turkey	[18]
Vertical GHE	Heating	Water	Turkey	Average system COP of 3	[19]
Double tube U-tube Multi-tube	Cooling	Water	China	Double U-tube exhibits best thermal performance	[20]
Vertical, Horizontal	Heating/ Cooling	Water	Cyprus	Vertical HE provides a higher potential	[21]
U-type GHE	Cooling	Water	Turkey	GSHP is more feasible that ASHP	[22]
Horizontal GHE	Cooling	Water	Tunisia	High cooling potential using GSHP in Tunisia	[23]
Open loop, Horizontal parallel GHE	Heating	Air	Poland	Ground heating provided 24% of total heating load	[24]
EAHE	Heating/ Cooling	Water	Brazil	Higher heating than cooling potential	[25]
Vertical Boreholes	Heating/ Cooling	Water	Spain	ASHRAE handbook over predict pipe length required	[26]
Vertical GHE	Heating/ Cooling	Water	Germany	Cooling potential is greater than heating	[27]
Horizontal EAHE	Heating/ Cooling	Air	Egypt		[28]
U-tube HE	Heating/ Cooling	Water	India	Higher heating potential than cooling	[29]
Single, Double U-tube HE	Heating/ Cooling	Water	France	Double U-tube is 30% more effective than single	[30]
Vertical Borehole	Heating/ Cooling	Water	China	COP of 3 and 3.2 for heating and cooling respectively	[31]

2.2. Mathematical Models

Man [32] presented a solid cylindrical source model that takes into consideration both the radial dimension and the heat capacity of the borehole. The increase in temperature was calculated using the 1-D model and results were found to lie between those obtained using classical line source model and hollow cylindrical model. An expression for a 2-D solid cylindrical source model was derived and showed a lower increase in temperature in comparison to the 1-D model [32]. Molina-Giraldo et al. [33] adopted a new approach for the thermal analysis of GSHPs by considering ground water flow and axial effects in the moving finite line source model. The results were validated against numerical rests for a borehole of 50 m depth. A good agreement was obtained indicating the reliability of the model. The influence of both parameters was significant with a greater emphasis on the effect of axial heat flow. Furthermore, moving finite linear source model was compared to moving infinite line source model and the variation between both was diminishing with increasing velocity [33]. Florides et al. [34] modeled the performance vertical and horizontal ground exchanger using a mathematical model that calculates heat flow in the fluid, grout, tubes and ground. Critical values regarding the horizontal heat exchanger of soil diffusivity and center to center distances were obtained as 9×10^{-6} m^2/s and 0.7 m respectively. The efficiency of vertical and horizontal heat exchangers was compared and the result indicated that they have comparable efficiencies [34]. Niu et al. [3] developed a 1-D Steady state model that couples mass and heat transfer to study the performance of an EAHE. Influence of design parameters including air temperature, relative humidity, velocity as well as the tube length and diameter was investigated. The results are shown in Figure 2.1. At any given length, the temperature and humidity levels were found to be lower for a smaller pipe diameter [3].

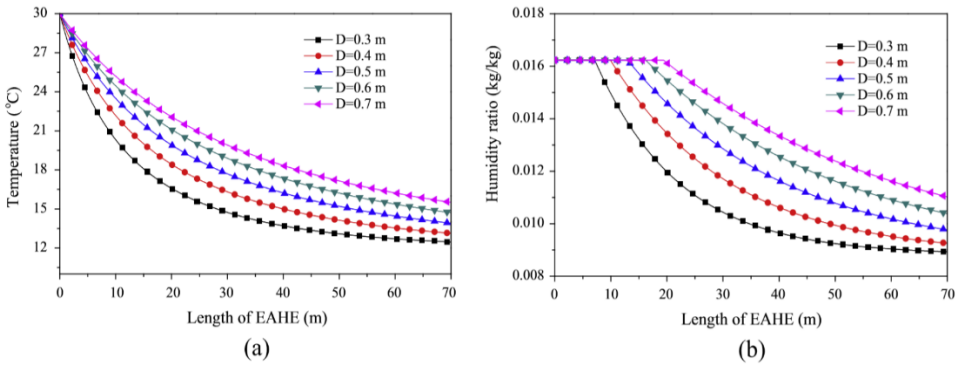

Figure 2.1: Performance of EAHE under the different tube diameter conditions [3].

Bisoniya [35] developed a one-dimensional mathematical model that aids in the initial design of an EAHE. Simple design equations that consider the Earth's Undisturbed Temperature (EUT), friction factor and Nu number improved the accuracy of the heat transfer calculations. The key assumptions made in developing this model include an initial ground surface temperature equal to that of the ambient air, EUT approximated to the average temperature of the location, neglecting the pipe thickness, and a uniform pipe surface temperature in the axial direction [35]. To evaluate the overall performance a J- factor was suggested as an indicator which is calculated as follows:

$$J = \frac{\Delta P}{NTU} \tag{1}$$

where $\Delta P = \left(\frac{fL}{D\rho}\right) * \frac{va^2}{2}$ and $NTU = \frac{hA}{m} c_p$

Kupiec et al. [36] presented a transient one-dimensional mathematical model with an internal source of heat. It was deployed to determine the rate of heat transfer between the ground and the working fluid in a horizontal ground heat exchanger. An m-stage cascade of perfect mixing tanks coupled with an upper exchanger was used to resemble the ground exchanger. The inlet and the outlet temperatures to and from the heat exchanger were defined as T_{Lo} and T_{Lm}, respectively. The ground temperature and the fluid temperature at different stages were defined as T_j and T_{Lj}. Thus, the rate of heat transfer at any stage was calculated using:

$$\dot{Q}_j = \dot{m}_L c_L \left(T_{Lj} - T_{Lj-1}\right) \tag{2}$$

The model was used to predict the deterioration in thermal performance of a horizontal ground heat exchanger under typical operation in the UK climatic conditions. It was concluded that a steady state is reached after 10 years of operation [36].

2.3. Numerical Models

Experimental studies are deemed as the most reliable in the field of research. However, given the high costs and imposed limitation researchers reside to numerical simulations. Three commonly used simulation tools included ANSYS Fluent, COMSOL and TRNSYS. Earlier studies utilized 2D models by imposing several assumptions while recent studies deployed 3-D models reducing the assumptions needed and producing more accurate results.

Demir et al. [37] developed a software in MATLAB to estimate fluid outlet temperature and the soil temperature distribution around a horizontal parallel pipe heat exchanger. The variation in soil temperature as a function of the climatic conditions was taken into consideration and the results were obtained for both heating and cooling mode then compared to the experimental data. A good agreement was obtained between numerical and experimental results with a maximum error of 10%. Soil thermal conductivity was observed to be the most influential parameter in terms of soil properties and the burial depth along with the distance between the pipes in terms of design parameters [37]. Li [38] presented a 3-D unstructured finite volume model adopting the Delaunay triangulation method for meshing, thus including the interior and exterior of the borehole. This numerical model was used to study the transient conjugate heat transfer occurring in a vertical U tube borehole on a short time scale. The operation of the heat exchanger was intermitting with a total operating period of 50 days. The model was validated against experimental data and showed good agreement [38].

Wu et al. [39] studied the thermal performance of straight and slinky horizontal heat exchangers. A 3-D model developed using FLUENT and validated against experimental results. The model was utilized to evaluate the thermal performance of slinky GSHP at different coil diameters and central interval distances. It was concluded that a larger coil diameter resulted in a higher heat extraction per meter length. Furthermore an increase in the central interval distance was associated with an increase in the specific heat extraction [39]. Bansal et al. [40] developed a transient model to mimic the thermal performance of an earth air heat exchanger. Operating parameters including pipe material and air velocity were varied. Cooling of 8 to 12°C was achieved using a 23.42 m long pipe. While the pipe material showed a negligible, influence on the cooling capacity a remarkable impact was observed due to the air velocity. Over sizing heat exchangers particularly in the case of slinky coil is common in practice which emphasizes on the necessity for finding an optimum design method [40].

Shang et al. [41] developed a numerical 3-D model was generated to predict the geo temperature distribution during intermittent operation of a ground source heat pump in the heating mode. FLUENT 6.3.26 was used to obtain results and study the effect of thermal conductivity, soil porosity, backfill material, air temperature, solar

radiation and wind velocity on the rate of recovery. It was concluded that the rate of temperature variation was higher initially and decreased with time. The influence of soil thermal conductivity, porosity, and backfill material was found to be significant in contrast to that of air temperature, solar radiation, and wind velocity. Understanding the impact of each factor is of major importance to maximize the rate of heat transfer and enhance the heat pump performance [41]. Benazza et al. [42] deployed an unsteady quasi 3-D numerical simulation to study the performance of a horizontal ground heat exchanger in the cooling mode. The boundary condition for the ground surface temperature was set to a harmonic function to account for the climatic conditions in Algeria. It was concluded that the heat flux reduces in the case of continuous operation in compared to cyclic operation at intervals of 8 or 16hours. Furthermore, the effect of soil thermal conductivity was found to have a higher significance in comparison to tube spacing and tube diameter [42].

Khalajzadeh et al. [43] derived a model for quantifying the total heat transfer efficiency and the heat exchanger efficiency using second-order Response Surface Model with the aid of the 3-D model CFD results. Dimensionless parameters were introduced to decrease the number of design parameters and their effect was studied on the total heat transfer and heat exchanger efficiency. The influence of the dimensionless inlet fluid temperature and dimensionless pipe diameter was found to be significant. In contrast, the effect of the dimensionless depth was found to be minimal [43]. Congedo et al. [44] investigated the energy behavior of horizontal ground heat exchangers with 3 different configurations. The heat fluxes transferred to and from the ground in the case of Linear, helical and slinky horizontal heat exchangers were compared. It was concluded that the helical configuration exhibits the best performance. Each case was studied at three different mass flow rates through varying the velocity (0.25, 0.5 and 1 kg/s). Furthermore, the effect of ground thermal conductivity around the heat exchangers was analyzed (1 to 3 W/m.K). Results obtained indicated that ground thermal conductivity has the greatest impact on the heat exchanger performance with 10 times the amount of heat transferred in the case of helical heat exchanger in comparison to linear and 5 times in comparison to slinky heat exchanger [44]. Fujii et al. [45] simulated the performance of a slinky coil horizontal ground heat exchanger. FEFLOW, a finite element simulator was used to predict the ground temperature

distribution after 38 days of operation at 20 hours per day. A decline in the rate of heat extracted was observed after 10 days indicating an increase in ground temperature [45].

Chong et al. [46] assessed the impact of varying loop pitches, loop diameters, and soil thermal properties by numerical simulation of a slinky loop heat exchanger. A 3-D model using FLUENT 13.0 was developed to simulate the performance of the ground heat exchanger given the UK climate conditions. Results indicated that loop pitch had a significant influence on the performance in contrast to loop diameter. In addition, a direct relation was observed between soil thermal diffusivity and the overall performance indicating the necessity of accurate evaluation of the soil properties. On the other hand, intermittent operation was compared to continuous operation. Under the 12 hours on and 12 hours off operation, a noticeably enhanced thermal performance was observed in comparison to the continuous operation over a period of 60 days [46].

Misra et al. [47] evaluated the performance of an EATHE (Earth Air Tunnel Heat Exchanger) in India for cooling applications. A 3-D model developed using ANSYS Fluent was used to assess the impact of several parameters on the thermal performance. The effect of soil thermal conductivity, pipe diameter, and flow velocity and time duration of continuous operation was studied under steady state and transient mode. A significant deterioration in performance was observed in the transient mode with a maximum of 64% derating. The deterioration was found to be greater in the pipes of larger diameter as a result of the air turbulence within larger pipes. This effect was not as noticeable in the cases of high soil thermal conductivity due to the faster rate of heat transfer [47]. Bisoniya et al. [48] created a geometry representing a pipe of 19.288 m length with a diameter of 0.1016 m, buried at 2 m of depth was developed using Unigraphics NX7.0. The simulation was carried using CFX 12.0 under steady state conditions. Air temperatures based on Indian climate conditions during summer and winter operation were applied as boundary conditions. The cooling potential was found to be higher than the heating potential at 247.25 kWh and 191.06 kWh respectively. The energy payback time for the proposed system operating at 5 m/s was found to be 1.29 years [48]. Bottarelli et al. [49] mixed encapsulated PCM (Paraffin) with backfill material surrounding the heat exchanger. A 2-D transient model was developed to study the thermal performance in heating and cooling modes. The introduction of PCM was assumed to enhance the thermal storage potential of shallow ground heat exchangers.

Results indicated an increase in the COP of the GCHP and a clear smoothing of the thermal wave generated by the heat pump[49]. Bidarmaghz et al. [50] developed a 3-D model using COMSOL to simulate the heat transfer in the ground coupled to 1-D heat transfer and fluid flow in the pipes of a U-loop HE. The main contribution was investigating the effect of surface thermal recharge on the heat exchange rate. It was concluded that the minimum average pipe wall temperature was 1°C lower when the surface effects were not considered. In addition, considering surface effects was found to be of a greater impact in the case of shallower boreholes with a reduction of 11% for the 30 m depth heat exchanger and 6% for the 50 m depth HE [50].

Congedo et al. [51] modeled the performance of an EAHE in Otranto, Italy which is identified by its hot and humid climate. Using ANSYS Fluent, the system was modeled taking into consideration humidity levels. EAHE of 5 m length was found to provide 23 kWh of cooling in the winter and 37 kWh in summer, thus it's an attractive ventilation solution particularly for passive houses. It was concluded that post treatment using the heat pump can be avoided particularly during the summer. Furthermore, the best performance was obtained at a depth of 5m and a soil thermal conductivity of 3 W/m.K [51]. Bortoloni et al. [52] developed a transient 2-D simulation using COMSOL to establish an understanding of the most suitable ground surface boundary condition. The three boundary conditions compared include ground surface energy balance, heat flux and temperature on ground surface. It was concluded that setting the ground surface temperature as a boundary condition produces the most accurate results given that it was estimated correctly [52].

Sangi [53] studied the feasibility of utilizing Modelica to simulate the actual performance of slinky-coil horizontal ground heat exchanger. Conduction was considered to be the governing heat transfer mechanism in the soil sub-model while convection and radiation were neglected. In the pipe sub-model, two heat transfer mechanism were considered dominant heat conduction and heat convection. To validate the proposed model, simulation results were validated against experimental results published in Japan. The agreement between simulation of the two models developed and experimental verified the validity of the model [53].

Table 2.2: Numerical Studies.

Configuration	**State**	**Mode**	**Location**	**Tool**	**Reference**
Horizontal parallel pipe	2D, Transient	Heating/ Cooling	Turkey	MATLAB	[37]
Vertical U-tube	3-D, Transient	Cooling	China		[38]
Straight, Slinky Horizontal	3-D, Transient	Heating	UK	Fluent	[39]
Horizontal pipes	3-D, Transient	Cooling	India	Fluent	[40]
Vertical U-tube	3-D, Transient	Heating	China	FLUENT	[41]
Horizontal GHE	3-D, Transient	Cooling	Algeria		[42]
Vertical U-tube	3-D, Transient	Cooling	Iran	FLUENT	[43]
Linea, Helical slinky Horizontal	3-D, Transient	Heating/ Cooling	Italy	Fluent	[44]
Slinky coil Horizontal	3-D, Transient	Heating/ Cooling	Japan	FEFLOW	[45]
Slinky loop Horizontal	3-D, Transient	Heating	UK	Fluent	[46]
EATHE	3-D, Transient	Cooling	India	FLUENT	[47]
Horizontal EAHE	3-D, Transient	Heating/ Cooling	India	CFX	[48]
Horizontal GHE	2D, Transient	Heating/ Cooling	Italy	COMSOL	[49]
Double U-tube loop GHE	3-D, Transient	Heating/ Cooling	Australia	COMSOL	[50]
Horizontal EAH	3-D, Transient	Cooling	Italy	FLUENT	[51]
HGHE	2D, Transient	Heating/ Cooling	Italy	COMSOL	[52]
Slinky coil Horizontal	3-D, Transient	Heating/ Cooling	Japan	Modelica	[53]

2.4. Configuration

2.4.1. Vertical heat exchangers. Zarrella et al. [54] analyzed the thermal performance of helical and triple U-tube heat exchangers shown in Figure 2.2 by developing a numerical CaRM model. The advantage of adopting the helical configuration over triple U-tube was obvious with 23% increase in thermal performance at peak load. However, that was countered with a significantly higher pressure drop associated with the helical configuration. Furthermore, the influence of varying the pitch between the turns in the helical configuration was studied. Increasing the pitch from 0.15 m to 0.3 m was reflected as a 14% decrease in peak load [54].

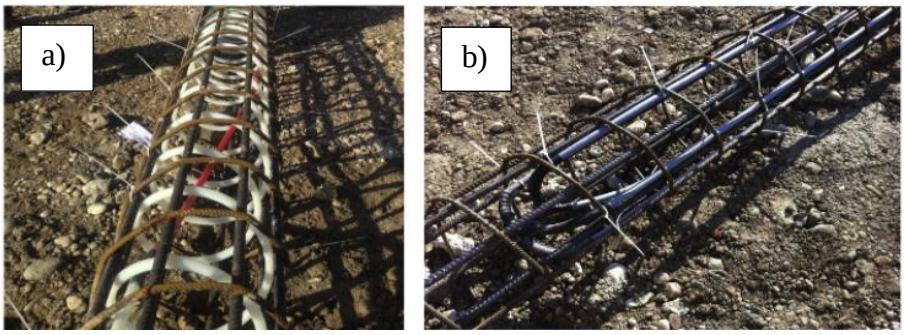

Figure 2.2: (a) Helical U-tube (b) Triple U-tube [54].

Park at al. [55] compared the thermal performance and ease of constructing several U-tube, S-shaped and coil type heat exchange pipes as illustrated in Figure 2.3. Six cast-in-place concrete energy piles were constructed, and the borehole effectiveness was evaluated. The time required for construction was reported as follows from longest to shortest: 8-pair and 10-pair U-type, coil type, followed by S-type heat exchange pipe. However, the optimum configuration interns of economic feasibility and thermal performance was obtained using the coil type heat exchange pipe [55].

Figure 2.3: (a) 5-pair-parallel U-type (b) 10-pair-parallel U-type (c) S-type [55].

Zhao et al. [56] conducted a comparative analysis on three types of heat exchangers Spiral shaped, W-shaped and U-shaped heat exchangers as displayed in Figure 2.4. A numerical model based on the finite element method was developed to

evaluate the thermal performance of each configuration. The performance over a period of 3 years was modeled and the thermal loads were found to reach their peak at the end of heating and cooling seasons. In contrast to the W shaped and U-shaped heat exchangers, spiral-shaped was found to have a uniformity distributed change in temperature thus exhibiting the best thermal performance on long and short term [56].

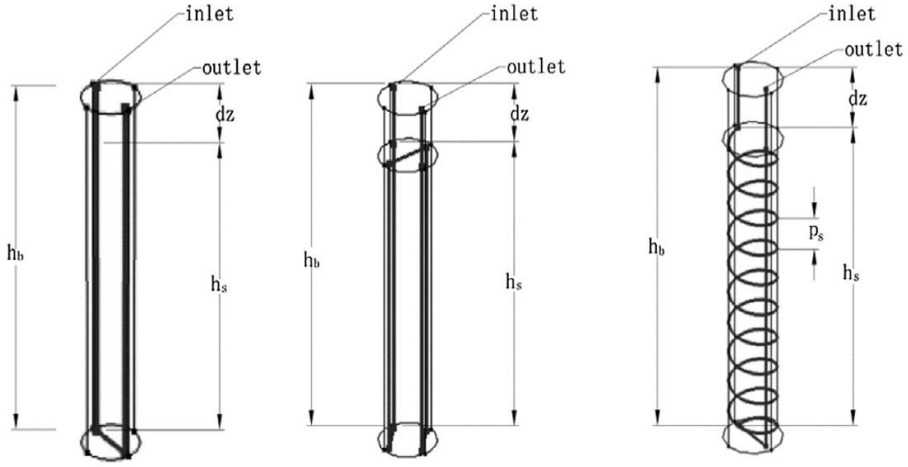

Figure 2.4: (a) U-shaped tube (b) W-shaped tube (c) Spiral-shaped tube [56].

Dehghan [57] compared the performance of linear-quadrilateral and circular configuration with 1 and 9 GHEs numerically and experimentally. The thermal performance of the linear configuration was found to be higher than circular by 5% for 1 GHE and 1% for 9 GHEs. On the other hand, the space occupied by the circular configurations was found to be less in comparison to linear configurations by 21%. The use of 9 GHEs was deduced to be more efficient in the case of cooling and maintaining a distance of 6 m between spirals was recommended [57].

Quaggiotto et al. [58] utilized numerical simulation to compare the thermal behavior of coaxial and double U borehole on the long-term and short-term run. A numerical tool CaRM was used to predict the thermal behavior in each case subjected to a balanced thermal load. The coaxial heat exchanger exhibited a higher rate of heat exchange in both the cooling and the heating mode in comparison to double u-tube. That was related to the large volume of the probe and the lower borehole thermal resistance [58]. Javadi et al. [59] compared the thermal performance of eight helical heat exchangers shown in figure X to the single U-tube heat exchanger with the same heat transfer area. The main parameters considered were heat exchange rate, pressure

drop, thermal resistance, and effectiveness. The triple helix resulted in the maximum variation in the working fluid temperature although its thermal resistance is equivalent to that of W-tube and double helix heat exchangers. An increase in number of coils was associated with an increase in pressure drop, thus the only advantage of single U-tube heat exchangers is the lower pressure drop [59].

2.4.2. Horizontal heat exchangers. Yoon et al. [60] experimentally evaluated the rate of heat exchange of horizontal slinky, spiral-coil and U-type GHEs through conducting thermal response tests. The test was carried in a 5×1 steel box and results were used to perform a cost-efficiency analysis. Overall, U-type GHE exhibited the best performance followed by spiral-coil GHE with a 30−40% heat exchange rate greater than that of slinky GHE. A similar trend was observed while comparing the cost-efficiency analysis with U-type showing an economic efficiency 20% greater than that of spiral and slinky [60].

Kim et al. [2] investigated the performance of coil type and slinky type horizontal GHEs numerically and experimentally. Numerical analysis was deployed to evaluate the magnitude of impact of each of the design parameters on the thermal performance. While the influence of soil thermal conductivity and type of GHE was found to be significant the pipe diameter was found to have no effect. Furthermore, a steel boxes used to conduct the thermal response test on both configurations. The performance of coil type GHE was found to surpass that of slinky type GHE by 10−11% regardless of soil conditions [2].

Selamat et al. [61] examined design optimization of a horizontal ground heat exchanger. Four different configurations displayed in Figure 2.5 were compared in terms of pressure drop, rate of heat exchange, effective period and thermal interference. 3-D models developed in ANSYS FLUENT 14.5 where used to simulate the performance of each configuration in the cooling mode over a period of 5 days. Slinky heat exchangers were found to exhibit a longer period of effective heat transfer in comparison to straight heat exchangers. Furthermore, the vertical orientation was found to extend the effective period by 14% and a pipe material study showed an improved performance with the use of copper pipes in comparison to HDPE [61].

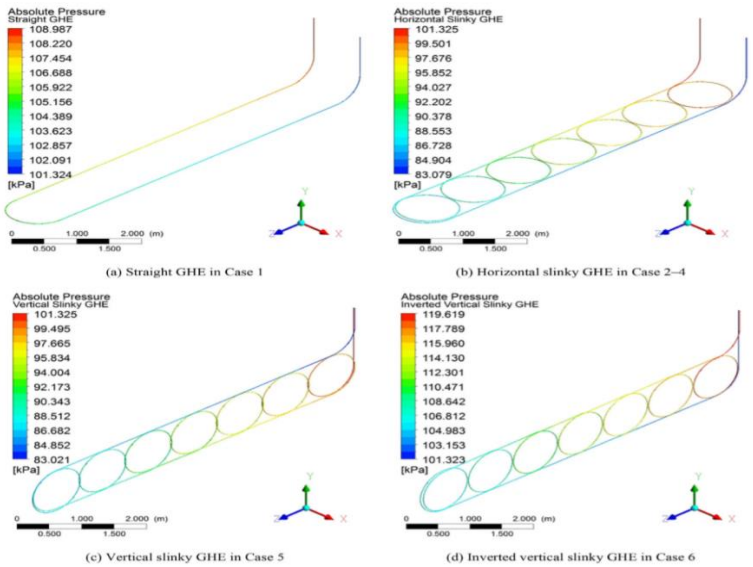

Figure 2.5: Pressure distribution in the four main GHE layouts [61].

M. Habibi and A. Hakkaki-Fard [62] developed a 3-D numerical model to evaluate the thermal performance and initial cost of 4 horizontal ground heat exchanger configurations. The study considered linear, spiral, horizontal and vertical slinky in single and parallel configurations. In the case of single arrangement, linear configuration exhibited the highest rate of heat exchanged per pipe unit length. The spiral configuration was found to have the lowest initial installation cost for the single arrangement. On the other hand, linear configuration was found to have the lowest initial installation cost for the parallel arrangement. Furthermore, the effect of varying the secondary soil moisture content on the rate of heat exchanged was studied for ordinary soil and sandy soil. The impact of the normalized soil water contents (Sr) was considered and result show an enhanced performance with increase in moisture except at the end of the winter season as shown in Figure 2.6 [62].

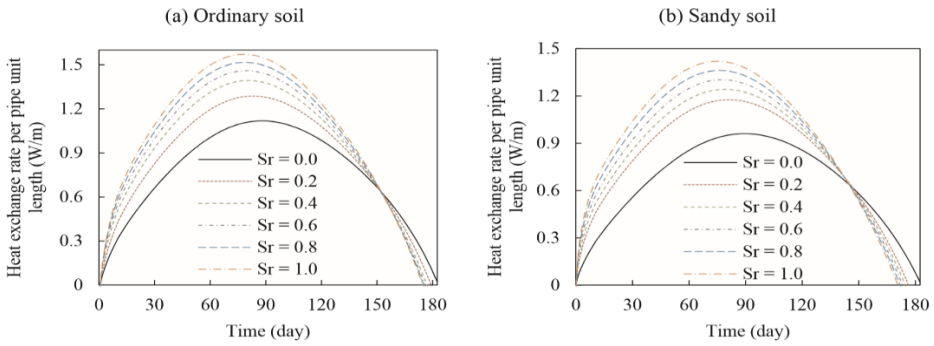

Figure 2.6: The effect of moisture content of secondary soil on thermal performance of spiral type of GHE in parallel configuration [62].

2.5. Performance Parameter

Performance of a heat exchanger is dictated by the value of several factors. The magnitude of impact of each of these parameters varies depending on the configuration and mode of operation. Numerical and experimental studies were deployed to evaluate the influence of burial depth, flow velocity, pipe diameter, pitch, and several other factors on the performance. Maximizing thermal performance and minimizing installation and operational costs are generally targeted when designing the heat exchanger. All of the Numerical studies below were validated against experimental results and showed good agreement.

2.5.1. Vertical heat exchangers. A. Zarrella and M. De Carli [63] analyzed the thermal behavior of vertical ground heat exchanger with helical pipe using a numerical model. Heat transfer in this process was presented as a network of resistors and capacitors. The configuration was effective for applications with low heating and cooling demands. The model took into consideration the influence of external air temperature, incident solar radiation and radiant heat exchange with the sky. A parametric study compared the effect of weather conditions, axial heat transfer, pitch between turns and type of ground on the thermal performance. Weather conditions exhibited the greatest influence in contrast to pitch between the turns [63]. F. Robert and L. Gosselin [64] performed an economic analysis using a mathematical model to study the effects of the number of boreholes, borehole length, spacing and peak load ratio. In addition, the effects of ground thermal conductivities and system loads were considered. The parameters with greatest impact on cost were found to be the number of boreholes and their depth [64]. Pu et al. [65] evaluated the thermal and pressure performance of a vertical U-tube heat exchanger numerically. The influence of varying the Reynolds number, pipe diameter and tube connection configurations was studied. A dimensionless evaluation criterion that considers thermal and pressure performance was proposed. Increasing the Reynolds number was found to enhance the performance under laminar flow condition. The influence of the tube diameter was minimal, and the parallel configuration outperformed series connection [65].

2.5.2. Horizontal heat exchangers. R. R. Dasare and S. K. Saha [66] proposed a method of designing horizontal ground heat exchangers for high energy demand applications. Using the numerical model developed for each of the configurations

(linear, helical and slinky) the relative significance of operating parameters was deduced. Results obtained are summarized in 4 graphs as shown in Figure 2.7.

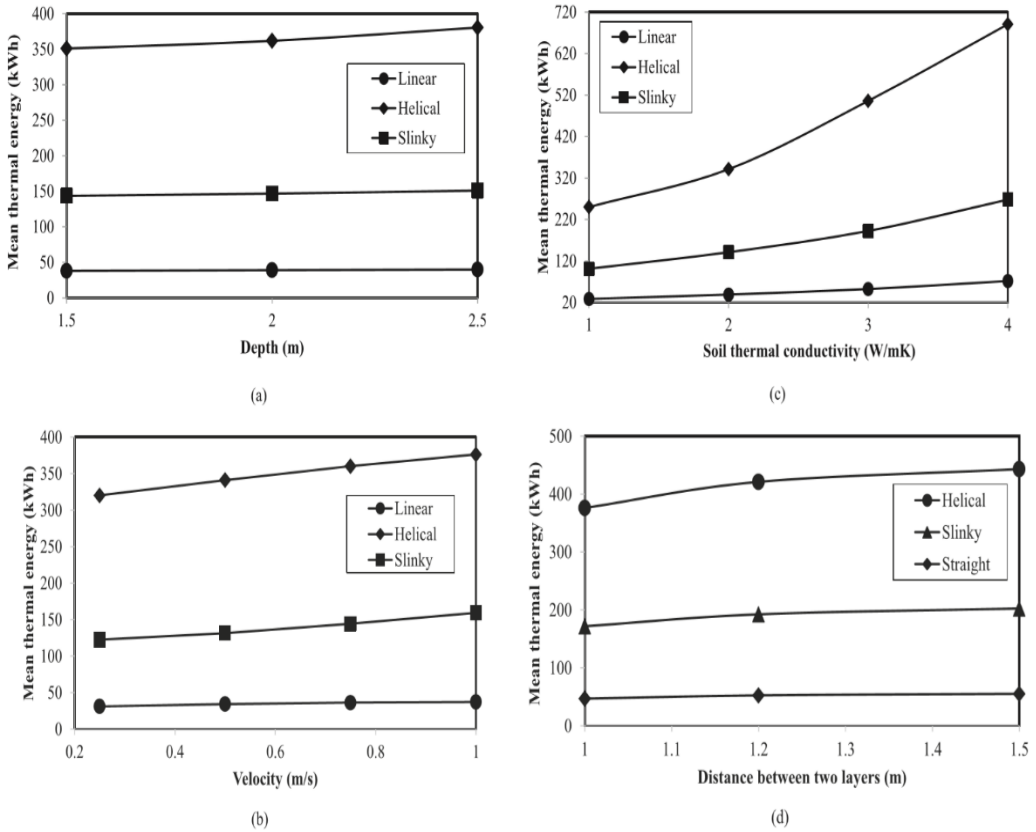

Figure 2.7: Mean thermal energy transferred for (a) installation depth, (b) velocity of heat transfer fluid, (c) soil thermal conductivity (d) distance between two layers of double layer ground heat exchanger [66].

Soil thermal conductivity along with fluid velocity were found to be very important parameters in contrast to installation depth which exhibited low significance. The results were used to design a new configuration (double layer helical geometry) which exhibits high thermal performance at low cost through combining horizontal and vertical ground heat exchangers [66].

Dehghan et al. [67] utilized COMSOL to study the influence of pitch distance, major distance and pitch length on the performance of a helical heat exchanger. Results indicated that a 100% change in length and diameter of a pitch can improve the performance of the HE by 10% at the expense of increasing the cost by more than 10%. In general, spacing was found to be the most influencing parameter and must be optimized based on number of GHEs and operational time [67]. N. Kayaci and H. Demir [68] utilized a numerical model to study the long-term effect on soil temperature

in the heating mode. Over a period of 10 years, the performance of a HGHE in Turkey was simulated and the transient soil temperature profile was applied. The effect of burial depth, distance between pipes and surface effects on soil temperature distribution were investigated. Increasing the spacing between the pipes beyond 2 m didn't have any influence on the soil temperature and the effects of surface conditions were more obvious at burial depths of less than 1 m. At the end of the 10 years period the soil temperature was found to decrease by 0.7°C. Furthermore, the soil temperature profile was found to become steady periodic after 5 year of operation [68].

Zarrella et al. [69] studied the performance of short helical ground HEs at three operation modes: daytime, nighttime and intermittent operation in Italy. Preference of operation mode was found to be season dependent with daytime being preferable during heating and nighttime during cooling. Two different grout materials were compared with a thermal conductivity of 2.5 W/m.K and 1.5 W/m.K, the best performance was obtained using the thermally enhanced grout operating in the intermittent mode [69]. Pu et al. [70] performed a parametric study numerically evaluating the impact of each parameter on the thermal performance of a horizontal ground heat exchanger. Four main parameters were considered including bending number, layout, pipe spacing and buried depth. The bending number is 0 for a single pipe and 1 for a U-type, pipes with bending numbers 0, 1, 3, 5 and 7 were studied. Single pipe outperformed bending pipes due to the absence of thermal interference but is undesirable due to high length to width ratio. Staggered layout was compared to in line arrangement, if the relative offset distance was higher than $1/3$the staggered arrangement exhibited better performance. The critical pipe spacing required to avoid interference was found to be a function of Tin, Re, and buried depth [70]. Wu et al. [71] developed a 2-D transient model using Fluent to study the thermal performance of a horizontal ground heat exchanger buried at a depth of 1.8 m in the UK climate conditions. Contribution of each of the performance parameters was evaluated including ambient air temperature, wind speed, refrigerant temperature and soil thermal properties. An increase in ambient air temperature and soil thermal conductivity was correlated with an enhanced rate of heat extraction. The opposite was observed when increasing the refrigerant temperature, while wind speed didn't result in any significant effect [71].

Table 2.3: Parametric Studies.

Configuration	**Parameters studied**	**Parameter of greatest influence**	**Optimization objective**	**Reference**
Vertical helical shaped pipe	Weather conditions, axial heat transfer, pitch between turns and type of ground	Weather conditions	Thermal performance	[63]
Vertical HE	Number of boreholes, Borehole length, spacing, and peak load ratio	Number of boreholes	Cost	[64]
Vertical U-tube HE	Reynolds number, tube diameter, and tube connection configuration	Reynolds number	Thermal performance and cost	[65]
Horizontal (linear, helical, slinky) HE	Soil thermal conductivity, Fluid velocity, Installation depth, and distance between 2 layers of double layer HE	Soil thermal conductivity	Thermal performance and cost	[66]
Helical GHE	Pitch distance, major distance and pitch length	Pitch distance	Thermal performance and cost	[67]
Horizontal GHE	Burial depth, distance between pipes, and surface effects	Burial depth	Soil Temperature	[68]
Helical pipe HE	Operation mode, grouting material, diameter of HE		Thermal performance and cost	[69]
Horizontal GHE	Bending number, layout, pipe spacing, and burial depth	Bending number	Thermal performance	[70]
Horizontal GHE	Ambient air temperature, wind speed, refrigerant temperature and soil thermal properties	Soil thermal conductivity	Thermal performance	[71]

Replicating heat exchanger design in different locations will yield different outcomes. That's mainly attributed to the difference in ground temperature distribution and thermal properties. Based on several studies soil thermal conductivity which is a factor of soil thermal diffusivity exhibits the greatest impact on the rate of heat exchanged. Thus, numerous studies reported soil thermal conductivity values in various regions. Those were obtained experimentally or mathematically through heat transfer models. Soil thermal conductivity is also a function of ground temperature, which varies with depth and time. Several models applying energy balance at the surface and studying heat conduction in the ground aimed to predict the ground temperature distribution. Depending on the number of input parameters required the accuracy and complexity of the model varied.

2.6. Ground Temperature Distribution

Estimating the correct ground temperature is of a great importance to avoid over sizing or under sizing the heat exchanger. Several studies attempted to develop a model that can accurately estimate ground temperature distribution. Key assumptions commonly adopted include constant soil thermal diffusivity, homogenous soil, undisturbed soil temperature equal to that of average air temperature and One-dimensional heat transfer. Deploying such assumptions reduce the need for several input parameters at the expense of the model precision. Droulia et al. [72] developed an analytical model by assuming an infinite depth of soil with an initial uniform temperature Tin. A semi-empirical model was obtained by replacing the constant Ta in the analytical model by a variable. Thus, the results of the semi empirical model fluctuate in a more realistic way in comparison to analytical. However, both showed good correlation with experimental data despite the minimum input data required. The analytical model applied to estimate soil temperature is presented in equation (3).

$$\begin{aligned} T(z,t) = T_a &+ A_1 e^{-\frac{z}{d_1}} \sin\left(\left(\frac{2\pi t}{8760}\right) + \varphi_1 - \frac{z}{d_1}\right) \\ &+ A_2 A_3 e^{-\frac{z}{d_2}} \sin\left(\frac{2\pi t}{24} + \varphi_3 - \frac{z}{d_2}\right) \\ &- A_2 e^{-\frac{z}{d_3}} \sin\left(\frac{364.2\pi t}{8760} - \varphi_2 + \varphi_3 - \frac{z}{d_3}\right) \\ &- \left(\frac{A_2}{2}\right) e^{-\frac{z}{d_4}} \sin\left(\frac{364.2\pi t}{8760} + \varphi_2 + \varphi_3 - \frac{z}{d_4}\right) \end{aligned} \quad (3)$$

in which d_1, d_2, d_3 and d_4 are constants associated with diffusivity noted as D with $d_1 = \sqrt{\frac{D.8760}{\pi}}$, $d_2 = \sqrt{\frac{D.24}{\pi}}$, $d_3 = \sqrt{\frac{D.8760}{364\pi}}$, $d_4 = \sqrt{\frac{D.8760}{366\pi}}$ and the variables D, A_i and φ_i (i =1, 2, 3) were obtained through nonlinear regression [72].

Ozgener et al. [73] developed a model that predicts the ground temperature distribution as a function of depth and time. Deploying the assumptions of One-dimensional heat flow and constant soil properties to predict the temperature at a depth of 5 cm, 10 cm, 20 cm and 300 cm. Results obtained using equation (4) to calculate ground temperature as a function of depth z, were validated against measured data from a setup in Izmir, Turkey.

$$T(z,t) = T_m + A_z \sin\left[\frac{2\pi}{P}(t - t_o) - \gamma z - \frac{\pi}{2}\right] \quad (4)$$

WhereT_m is the mean surface temperature and $A_z = A_0 e^{-\gamma z}$ with γ defined as the damping depth and calculated as $\gamma = \sqrt{\frac{\pi}{\alpha P}}$,where P is the period of oscillation and $\alpha$is the soil thermal diffusivity and t_o is the time needed for the surface soil temperature to reachT_m. Utilizing the above model, the lowest error was obtained at 10 cm depth. Although the error was generally with the acceptable range. It was suggested that deploying measured daily soil surface temperatures instead of daily air temperature would yield better results. The three main parameters involved in calculating the ground temperature distribution include the annual average ground surface temperature, annual amplitude of ground surface temperature and phase angle [73]. C. O. Popiel and J. Wojtkowiak [74] developed a semi-empirical model based on the analytical solution of a 1-D transient temperature distribution in a semi-infinite solid and data collected in Poznan, Poland. Measurements of ground temperature revealed a consistence in air and ground temperatures for depth less than 0.35 m during the summer and 0.1 m during the winter. The measurements were recorded in two locations, grass and bare ground. It was found that grass is more suitable given the temperatures obtained at 1.5 m during both seasons. The equation developed to predict the ground temperature distribution included three empirical coefficients. The result obtained were 95% accurate in comparison to measured temperatures. Thus, the model was said to be valid for regions with climatic conditions similar to those of central Europe [74].

G. Tsilingiridis and K. Papakostas [75] investigated the relation between ground temperature and ambient air temperature using data recorded over a period 10 years. Thermometers placed in Northern Greece a depth of 0.5, 1 and 1.5 m, in two locations, grass and bare land. The difference in air and ground temperature was found negligible at shallow depths above 0.5 m, while it was found to be between 5 and 10°C at a depth of 1.5 m during the winter. For each depth and time period a correlation was developed to estimate the ground temperature [75].

From August to January (I):

$$T_{gr,0.50} = 0.0116 \times T_a^2 + 1.4289 \times T_{air} - 0.3515, \qquad R^2 = 0{,}9892 \qquad (5)$$

From February to July (II):

$$T_{gr,0.50} = 0.0106 \times T_a^2 + 0.6737 \times T_{air} + 3.0285, \qquad R^2 = 0{,}9920 \qquad (6)$$

From August to January (I):

$$T_{gr,1.00} = -0.0213 \times T_a^2 + 1.5148 \times T_{air} + 1.8881, \qquad R^2 = 0{,}9772 \qquad (7)$$

From February to July (II):

$$T_{gr,1.00} = 0.0196 \times T_a^2 + 0.1856 \times T_{air} + 7.3637, \qquad R^2 = 0{,}9844 \qquad (8)$$

From August to January (I):

$$T_{gr,1.50} = -0.0263 \times T_a^2 + 1.4740 \times T_{air} + 4.3049, \qquad R^2 = 0{,}9621 \qquad (9)$$

From February to July (II):

$$T_{gr,1.50} = 0.0233 \times T_a^2 - 0.1220 \times T_{air} + 10.6790, \qquad R^2 = 0{,}9757 \qquad (10)$$

H. Xu and J. D. Spitleret et al. [76] developed a 1-D numerical model and introduced factors that are often neglected in the calculation of ground temperature distribution such as moisture transfer, soil freezing and snow cover. It was concluded that the contribution of snow coverage and soil freeze was high in contrast to that of moisture transport. Results obtained using the model were validated against measurements of temperature for 3 locations in Montana and showed good agreement. However, the model was only validated against data from green field with fine grained soils thus may not be applicable otherwise [76].

Ouzzane et al. [77] developed two correlations of the undisturbed ground temperature using measured data from 17 sites. One of the correlations as a function of air temperature, wind velocity, sky temperature and solar radiation on a horizontal

surface. The coefficient of determination using this correlation was found to be 0.998. The correlation developed to calculate the ground temperature is as follow:

$$T_g = 1.205T_{amb} - 0.201T_{sky} - 0.466V_w + 0.0049Q_{sol} \quad (11)$$

Where T_{amb} is the ambient temperature, T_{sky} is the sky temperature, both in Kelvin,$V_w$is the wind speed and $Q_{sol}$is the solar radiation. The contribution of each parameter to the undisturbed temperature was evaluated and ambient air temperature was found to be dominant. Based on that a second correlation which is a simplification of the first was developed and is only a function of air ambient temperature. The coefficient of determination using the simplified correlation was 0.992 which is satisfactory [77].

$$T_g = 17.898 + 0.951T_{amb} \quad (12)$$

Soldo et al. [78] investigated soil properties and temperature distribution for 8 different sites in 2 regions in Croatia. Using distributed thermal response test which overcomes the need for the installation of several sensors by using a single fiber optic cable, the temperature profiles were obtained. Thermal properties, borehole resistance and undisturbed ground temperatures are compared for the inland, seaside and mountain regions. The undisturbed temperature varied between 10.58°C in the mountains to 16.17°C in the seaside. The borehole thermal resistance varied between 0.055 m.K/W to 0.154 m.K/W despite maintaining the same heat exchanger configuration. Thermal conductivity for soil in Dinaridic areas where carbonate rocks are dominate ranged between 2.01 and 3.19 W/mk, while Pannonia regions predominated with sediments had a soil thermal conductivity of 1.62−2.10 W/m.K [78]. Nikolaev et al. [79] supplemented the energy balance equation at the ground surface by an empirical correlation to predict the annual ground surface temperature. Thus, developing a model that is less sensitive to uncertainties from input factors. The results obtained were validated against measured data of sites in Montreal, Canada and two other sites in the U.S.A and showed good agreement. The solution was expressed in the form of Fourier series as shown in equation (13) [79].

$$T(z,t) = \overline{T_s} + Real \sum_{n=1}^{N} A_s \, e^{inwt - z\gamma - \emptyset_n} \quad (13)$$

where $\gamma = \frac{1+i}{\acute{\delta}}$ and $\acute{\delta} = \sqrt{\frac{2\alpha}{n\omega}}$. Where n is the number of the harmonic, t is the number of the day, A_s is the amplitude of the n^{th} harmonic and is equal to $\sqrt{a_n^2 + b_n^2}$, $\emptyset_n = Arctan\left(\frac{a_n}{b_n}\right)$.

The Fourier coefficients a_n and b_n are calculated as follows:

$$a_n = \frac{2}{365}\sum_{j=1}^{365} T(t)\sin(n\omega t) \quad (14)$$

$$b_n = \frac{2}{365}\sum_{j=1}^{365} T(t)\cos(n\omega t) \quad (15)$$

2.7. Soil Thermal Conductivity

Soil thermal conductivity is a function of many parameters including water content, particle shape and size, porosity, dry density and temperature. The precision of analytical models used to predict the soil thermal conductivity depends on the accuracy of those parameters. Empirical models on the other hand are easier to incorporate as their precision depends on the accuracy of experimental measurements but are only applicable for specific soil types under certain conditions. Thus, several studies reported soil thermal conductivities values of samples tested using steady or transient methods.

Nikolaev et al. [80] investigated the relation between soil thermal conductivity and temperature for 2 types of soil over a range of water content. Experimental data which was obtained by a steady state method called GHP, was fitted to develop an empirical relation. For both samples the thermal conductivity varied in 3 stages with respect to water content. A minor increase was noticed up to the wilting point and beyond the field capacity. However, a steep increase in thermal conductivity was recorded beyond wilting point and up to field capacity [80]. Barry-Macaulay et al. [81] tested the soil thermal conductivity of six soils and three rock types collected from Melbourne, Australia. Two methods were used for testing needle probe and divided bar apparatus. Thermal conductivity was studied over a range of water content, particle size, mineralogical composition and sample densities. Results indicated a positive relation between grain size, dry density, water content and soil thermal conductivity for all dry samples. However, when saturated no correlation was observed between density and thermal conductivity in Siltstone and sandstone in contrast to Basalt rocks. For dry

samples values ranged between 0.56 and 1.67 W/m.K while for saturated samples thermal conductivity ranged between 1.08 and 2.84 W/m.K [81].

N. Lu and Y. Dong [82] proposed a closed form equation capable of predicting the soil thermal conductivity of samples over a range of moisture contents at room temperature. Soil thermal conductivity λobtained using equation (16) showed good agreement with experimental results for unsaturated soils.

$$\frac{\lambda - \lambda_{dry}}{\lambda_{sat} - \lambda_{dry}} = 1 - \left[1 + \left(\frac{S}{S_f}\right)^m\right]^{\frac{1}{m}-1} \tag{16}$$

where $S_f$the degree of saturation, and m is defined as the pore fluid network connectivity parameter for thermal conductivity. The subscripts sat and dry refer respectively to the saturated and dry states [82].

F. Gori and S. Corasaniti [83] calculated the three-phase soil effective thermal conductivity by integration of the steady state heat conduction equation under thermal assumption of parallel heat flux along the z direction. The plane y-x of the 3-D cubic cell is shown in Figure 2.8 [83].

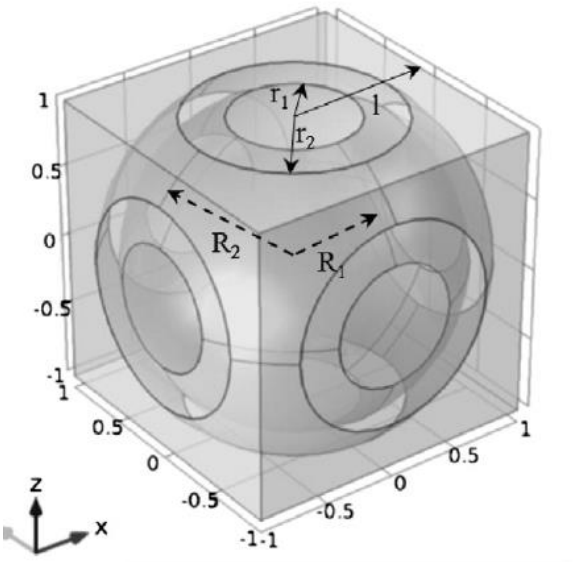

Figure 2.8: Elementary cell of the soil [83].

The model presented with a quasi-spherical solid grain for 3-phase media of soil, air, and water/ice was used to calculate the effective soil thermal conductivity as follows:

$$k = \frac{q_1 + q_2 + q_3 + q_4 + q_5 + 6}{2l\Delta T} \quad (17)$$

With q_1 as the heat flux crossing only the solid grain through a surface area of πr_1^2, q_2 crossing the series of liquid water, solid grain and liquid water through a surface equal to$\pi(r_2^2 - r_1^2)$, q_3 crossing series of air, liquid water, solid grain, liquid water and air through surface area equal to $\pi(l^2 - r_2^2)$, q_4 as heat flux crossing the series of air, liquid water, solid grain, liquid water and air through a surface area $=\pi(R_z^2 - l^2) - 4.[R_1^2.\arccos\left(\frac{1}{R_1}\right) - r_1.l]$, q_5 as heat flux crossing the series of air, liquid water, solid grain, liquid water, and air through a surface equal to $\pi(R_z^2 - R_1^2) - 4.\left\{\left[R_2^2.\arccos\left(\frac{1}{R_2}\right) - r_2.l\right] - \left[R_1^2.\arccos\left(\frac{1}{R_1}\right) - r_1.l\right]\right\}$, q_6 is crossing only air through a surface $\left\{4.l^2 - \left[\pi.R_2^2 - 4.R_2^2.\arccos\left(\frac{1}{R_2}\right) - 4.r_2.l\right]\right\}$.

Alrtimi et al. [84] proposed an empirical model capable of evaluating soil effective thermal conductivity as a function of porosity and water content. Steady state apparatus was used for testing the thermal conductivity of the Tripoli sand obtained from North Africa while controlling the boundary conditions [84]. Experimental results obtained were compared to those using existing models such as De Vries [85], Johansen, Côté and Konrad [86], Luet et al.[87], and Haigh model[88]. None of the models produced accurate results particularly at high levels of porosity and low saturation ratios. Thus, the model proposed was based on experimental results and was validated for samples of varying water content and porosity.

2.8. Hybrid-Coupled

2.8.1. Vertical heat exchangers. Man et al. [89] proposed a Hybrid Ground Coupled Heat Pump (HGCHP) for resolving the heat accumulation around a ground heat exchanger in cooling dominated regions. A 2-D transient hourly simulation model was developed to analyze the heat transfer in a HGCHP in comparison to GCHP. A cooling tower with a water flow rate of 1.2 m^3/h and an ambient air flow of 5000 m^3/h is used as a supplemental heat rejecter. Results indicated a higher borehole wall temperature in the case of traditional GCHP after 1 year of operation with an increase of 11°C in the base case and 18°C for the undersized GHE. This phenomenon of heat accumulation was omitted in the case of HGCHP with a wall temperature of an increase of 0.16°C after 1 year of operation. Thus, a reduction in both initial cost and operational

cost was achieved by deploying the HGCHP [89]. Wang et al. [90] investigated the advantages of adopting seasonal thermal storage during the summer in Harbin, China. The system consisted of a GCHP with solar collectors installed in a 3-story house that is 500 m^2 in area. The performance was monitored over one year to assess the performance of the system in severe cold climates. It was concluded that soil can be used as a heat sink directly for cooling without starting the heat pump. On the other hand, the solar collectors that are 50 m^2 in area were capable of supplying 49.7% of the total heating load thus increasing the COP of the system to 4.29 [90].

Xi et al. [91] optimized the design of a solar assisted ground coupled heat pump installed in Beijing, China by simulating a 20 years operation using TRNSYS. The land was divided based on the time of the year. Space heating represented the major load from November to April while domestic hot water was dominating in the rest of the period. A reduction in energy consumption for space heating of 5.6 GJ was achieved by integrating the solar collectors. Furthermore, a reduction in the borehole length of 3.67 m was associated with the addition of 1 m^2 of solar collectors. Overall, solar assisted heating and solar ground coupled heat pump modes were found to fulfill 22% of the total heating load [91]. Xi et al. [92] explored the performance of a solar assisted ground coupled heat pump at 4 operating modes experimentally. The study analyzed heat recovery and energy savings during continuous and intermittent operation for the case of SAGCHP and the traditional GCHP. Solar assisted heating exhibited a significant improvement in performance which was attributed to the higher borehole temperature. The best performance was achieved in the continuous 48 h space heating provided by both soil and solar energy as heat sources in the region of Shijiazhuang in China [92]. Man et al. [93] introduced a novel hybrid ground coupled heat pump with nocturnal cooling radiator (NCR) for air conditioning in cooling load dominated regions including subtropical areas. An analytical model was established to simulate the performance of the proposed system. The performance of each was studied over a period of 10 years for a 2-story building with a total area of 270 m^2. The borehole length required was decreased by 240 m with the addition of NCR area of 105 m^2. Results confirmed the feasibility of using NCR as supplemental heat rejecter particularly in buildings with limited land area. A total saving of 10.22 % over 10 years of operation was predicted based on simulation results [93].

Wang et al. [94] coupled evacuated tube solar collectors with a total area of 280 m^2 to a ground source heat pump supplying an office building with heating load dominating in Tianjin, China. The performance over a period of 50 years was simulated using TRNSYS and input parameters corresponding to those of the actual building were used. The average soil temperature of the BHE was found to decrease by 1.2°C after 50 years in contrast to that of the solar-assisted which annually increased the COP of the system. Therefore, it is said that such system is suitable in areas with a heating load far greater than the cooling load [94]. Rad et al. [95] assessed the feasibility of utilizing hybrid ground source heat pump with solar thermal collectors for heating in Toronto, Canada. Actual yearly data was compared to simulation results obtained using TRNSYS for a house in Toronto. It was concluded that introducing 6.81 m^2 of solar thermal collectors reduces the retired GHE length by 15% contributing to initial cost reduction. Thus, the hybrid system was found to be feasible and a 20-year LCC analysis showed that the net present worth of the hybrid system is 3.7-7% lower than the conventional system [95].

Fan et al. [96] proposed a design of a Hybrid ground source heat pump for an experimental study. The addition of a cooling tower and/or an Air Source Heat Pump for a cooling dominated building with a floor area of 476 m^2 situated in Shanghai, China was investigated. TRNSYS was utilized to optimize the performance of to omit heat accumulation which degrades the performance of the system. Various borehole depths were considered 60, 100 and 120 m along with two types of backfill material. Typical operating strategies were studied, and the minimum energy consumption was a result of combining 2 strategies (entering water temperature control and wet bulb temperature difference control). However, this reduction in energy consumption was at the expense of higher soil temperature [96]. Yang et al. [97] simulated the intermittent operation of a HGSHPP with double cooling towers using TRNSYS. Input parameters were based on the actual load of a hotel building based in Wuhan, China. Soil temperature was studied at different modes varying between continuous and intermittent. The best operating conditions were found to be in mode 3 in which the GHE is activated with cooling tower 1 on temperature control stagey followed by shutting down GHE, keeping cooling tower 1 On and cooling tower 2 on temperature control strategy. The addition of the second cooling tower was found to maintain the stability and reality of the system in case of GHE failure [97]. Dai et al. [98] studied the impact of heating

operation modes on the performance of a solar assisted ground source heat pump with 1 m^3 solar storage water tank. Six cases were investigated experimentally for enhanced soil temperature recovery rates. Results indicated that optimizing the recharging duration is crucial to avoid excess power consumption in the circulation pump. Furthermore, adding the solar thermal storage water tank aided in recharging at night with a significant impact on performance introduced by varying the flow rate through the tank. The optimum outcome for heating in Dalian, China was observed when connecting the Solar Heat Storage Water Tank in series with the GHE [98].

2.8.2. Horizontal heat exchangers. A. Chel and G. N. Tiwari [99] evaluated the performance of a 2.32 kWp PV integrated EAHE system over a period of one year. The total load on the system installed in Delhi, India was equivalent to 10 kWh/day and the performance of standalone PV system was compared to the building roof integrated PV system. The performance of the system was assessed by calculating the Energy conserved and tons of CO_2 mitigated from the existing setup. The annual saving potential in annual heating and cooling provided by the EAHE was found to be 3327 kWh/year and 2667 kWh/year respectively. Thus, a total of 9.4 tons of CO_2 is mitigated by the EAHE each year. While a PV system integrated with EAHE was found to mitigate 448 tons of CO_2 each year [99]. M. Maerefat and A. P. Haghighi [100] analyzed the cooling potential of a solar chimney combined with an earth air heat exchanger. The performance was a factor of outdoor air temperature, solar radiation, and configuration of solar chimney and EAHE. Optimizing the design of this system may aid in providing cooling demand for several hours, thus, such system is particularly interesting with standalone buildings [100].

Jakhar et al. [101] investigated the thermal performance of an EATHE experimentally and numerically using TRNSYS to as a function of inlet flow velocity, length of pipe and burial depth. A pipe of 60 m length buried at 3.7 m and air outlet temperatures were recorded for the base case and the system coupled with solar air heating duct (SAHD) as shown in Figure 2.9. The hybrid system produced higher outlet temperature (17°C) in comparison to 11°C using only the EATHE. Results indicate that for the same power consumption, the increase in the COP of the hybrid system of up to 6.304 which indicates the effectiveness of the system. The experimental and numerical results were in good agreement with a maximum variation of 8% [101].

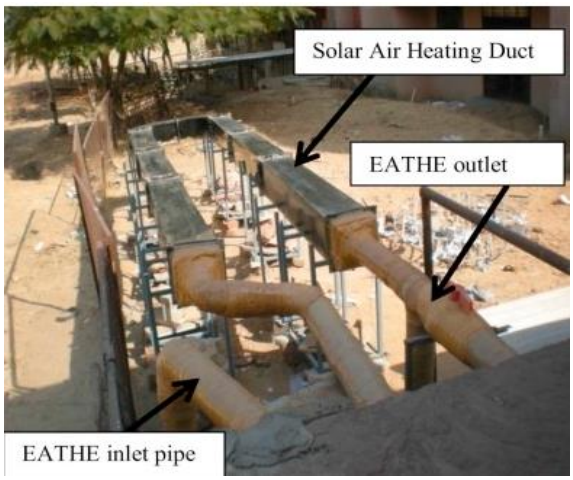

Figure 2.9: Solar Air Heating Duct coupled to Earth Air Tunnel Heat Exchanger [101].

Awani et al. [102] examined the potential of heating a 100 m^2 greenhouse shown in Figure 2.10 using a heat pump coupled to solar collectors and GHE in Tunisia. The solar collector was operated during daytime and disconnected at night when the GHE was operated. The ground temperature remained constant and high-water outlet temperatures were obtained. Thus, a great geothermal potential for heating exists in Tunisia. Furthermore, a numerical study showed a direct relation between system COP and size of solar collector with a maximum value of 5.5 [102].

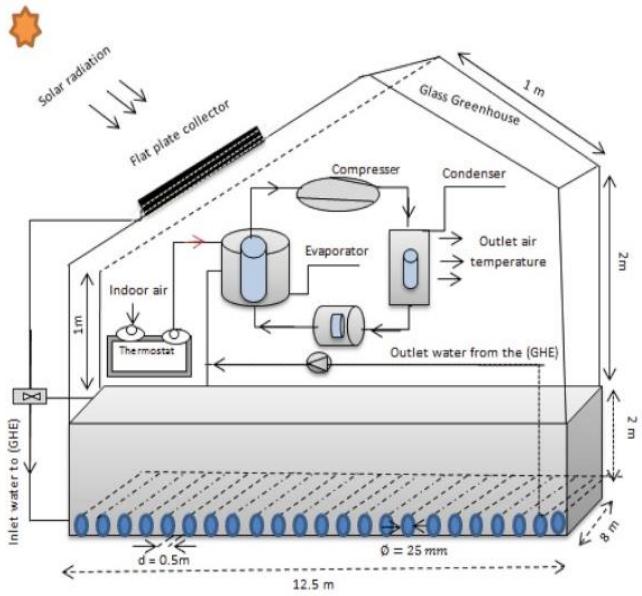

Figure 2.10: Schematic of the circulation system model [102].

Table 2.4: Hybrid coupled heat exchangers.

Configuration	**Mode**	**Supplemental**	**Reference**
Vertical U-tube	Cooling	Cooling tower	[89]
Vertical U-tube	Heating/ Cooling	Flat plate solar collector	[90]
Vertical U-tube	Heating	Flat plat solar collector	[91]
Vertical U-tube	Heating	Solar collector	[92]
Vertical U-tube	Cooling	Nocturnal cooling radiator	[93]
Vertical U-tube	Heating/ Cooling	Evacuated tube solar collector	[94]
Vertical U-tube	Heating	Solar thermal collectors	[95]
Borehole	Cooling	Cooling tower and ASHP	[96]
Vertical U-tube	Cooling	Cooling tower	[97]
Vertical U-tube	Heating	Evacuated tube solar collector +solar thermal storage	[98]
Horizontal EAHE	Heating/ Cooling	2.32 kWp PV	[99]
Horizontal GHE	Cooling	Solar chimney	[100]
EAHE	Heating	Solar air heating duct	[101]
Horizontal GHE	Heating	Flat plate solar collector	[102]

Chapter 3. Methodology

In this chapter, the performance of EWHE has been evaluated through four testing procedures. Firstly, soil physical properties are evaluated in lab to evaluate it thermal and physical properties. Second, Ground temperature has been measured over the course of 8 months (February 2019 till September 2019) using two bore holes. Third, experimental site has been constructed and tested with different water flow rates. Fourth, three-dimensional numerical simulations have been conducted to allow extrapolating on experimental data. Finally, a three-dimensional numerical model has been developed to relate mass flow rate, ambient temperature, EWHE size to EHWE performance.

3.1. Soil Physical Properties

The design of the ground heat exchanger is based on the geological formations and properties that dictate the thermal performance. Sample testing of the soil moisture content, composition and thermal conductivity is inevitable. Therefore, this information has been obtained from samples collected at depth of 2 m through lab testing.

3.1.1. Parameters testing setup. C-thermal analyzer was used to measure thermal conductivity utilizing Modified Transient Plane Source (MTPS) method, which has many advantages in comparison to other available testing methods such as guarded hot plate, hot wire or hot probe. The MTPS technique employs a one-sided, interfacial heat reflectance sensor that applies a momentary constant heat source to the sample after which the thermal conductivity is measured directly. Thermal grease paste has been applied as a contact agent on the surface of the sensor. A mold in the shape of a concentric cylinder has been placed over the sensor plate. The rise in temperature between the sensor and the sample induces voltage change in the sensor element, which translates into thermo-physical properties (thermal conductivities and heat capacity) of the sample.

3.1.2. Experimental procedure for soil thermal conductivity analysis. Parameters such as soil thermal conductivity, water content, heat capacity and latent heat dictate the way ground responds to variations in ground surface temperature. To investigate the effect of some of those parameters. Twenty samples have been prepared by fabricating a cylindrical mold, 4.2 cm in diameter and 5.1 cm in height. With 84

grams of as starting weight of dry sand, water has been added to make the weight percentage of sand range from 3% to 12%. The water is added to the dry weight of the sand at 3% increment. All samples have been observed to retain the same dimensions and thus it is clear that the only varying parameter is water content.

The samples are then taken to conduct thermal conductivity test after which each sample was physically compacted to produce five samples with different initial dry densities ranging from 1.4 to 1.7 g/cm^3. The thermal conductivity has been recorded for all the compacted samples.

3.2. Ground Temperature Measurement System

To produce a model that predicts the performance of an EWHE, the ground temperature over time is required. Given that the ground temperature is influenced by the meteorological elements including air temperature and solar radiation particularly at shallow depths, experimental setup is required to obtain the ground temperature for each geographical location.

To provide this data for the United Arab Emirates, two boreholes of 10 meters depth have been drilled within the American University campus, 7 thermocouples have been arranged on the surface of a PVC pipe embedded in the boreholes at depths of 0, 1, 2, 3, 5, 7, and 10 m as shown in

Figure 3.2. K- type thermocouples were used for temperature measurements, which were recorded hourly by Omega HH 309A data loggers.

The accuracy of the data loggers was $\pm$0.2% reading +1°C as indicated by the user manual. Thermocouples near the surface were placed at a distance closer to each other than those at deeper depths as solar radiation exhibits a greater influence at the surface. The effect of the solar radiation on ground temperature will vary based on the ground thermal conductivity and diffusivity.

The arrangement described was placed in two locations; one in a sandy area exposed to the sun, the other was placed in a shaded grassy area as shown in Figure 3.2. The purpose of varying the location was to analyze the effect of surface temperature and soil properties on ground temperature distribution. To evaluate the shading effect provided by the grass, that would insulate the surface, reducing the amplitude of temperature variation at the surface.

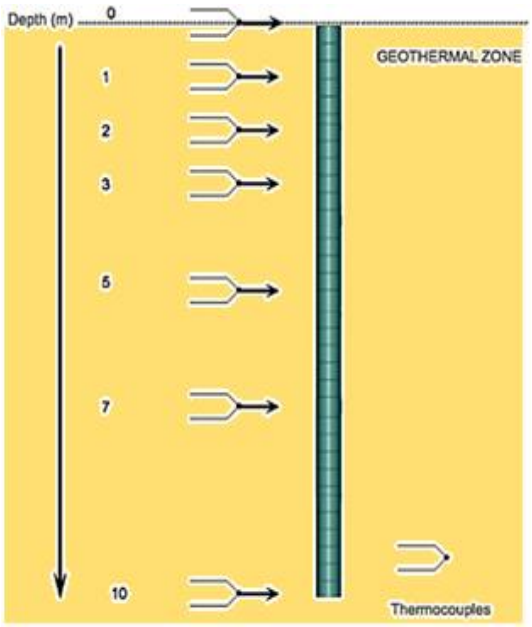

Figure 3.1: Schematic of thermocouples arrangement along the pipe.

Figure 3.2: Borehole setup (a) sand open exposed area (b) shaded grass.

3.3. EWHE Experimental Setup

To study the cooling potential of a EWHE, underground plastic pipes have been installed in parking 6 lot in the campus of the American University of Sharjah as shown in Figure 3.3. To investigate the thermal performance of the horizontal EWHE in the UAE, a trench of 2.5 m depth has been excavated as shown in Figure 3.4. The experimental set-up is shown in Figure 3.5 . The system consists of an EWHE connected to two tanks and a water heater. A 300 m long pipe which is made of polyethylene tube with 30 mm internal diameter has been buried at a depth of 2.5 m. The water heater capacity was 22 gallons and has been connected in series to two tanks, one with a volume of 200 gallons and the other of 100 gallons. A valve has been used

to control the flow and temperature sensors have been attached to record the inlet and outlet water temperatures as well as the ambient air temperature. Data has been collected using Omega HH 309Adata loggers with a time interval of 60s. In the described system, water has been circulated through the EWHE and heat has been released to the ground, since the water temperature is higher than the ground temperature. The properties of the pipe used in the setup is reported in Table 3.1.

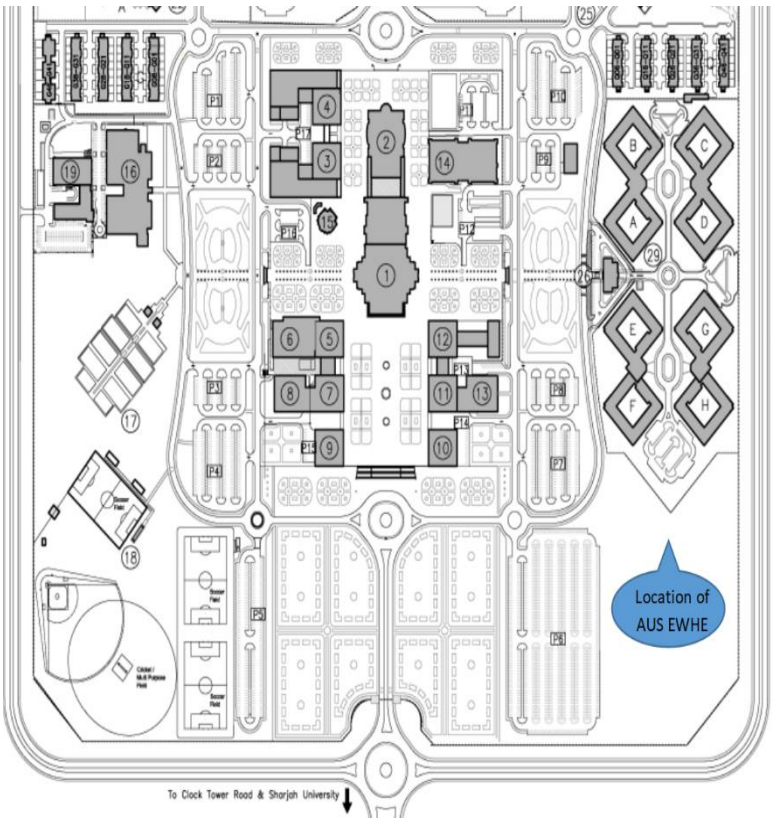

Figure 3.3: AUS map showing the location of the AUS EWHE.

Table 3.1: GHE configuration and properties.

Horizontal GHE	
Material	Cross-linked polyethylene
Length (m)	300
Inner diameter (m)	0.03
Pipe wall thickness (m)	0.0005
Thermal conductivity ($W.m^{-1}.K^{-1}$)	0.35

Figure 3.4: Trench of 2.5 m depth.

Figure 3.5: Trench setup.

3.4. Numerical Analysis

3.4.1. Governing equation. The current problem has been numerically simulated using commercial software ANSYS Fluent 19.1 that can analyze heat flow based on the finite volume method. Through applying the laws of conservation of mass, momentum and energy shown below, numerical simulation of the EWHE has been performed.

$$\nabla . v = 0 \qquad (18a)$$

$$\rho\left(\frac{\partial v}{\partial t} + v.\nabla\right)v = -\nabla p + \nabla.(\mu\nabla v) \qquad (18b)$$

$$\rho c_p\left(\frac{\partial T}{\partial t} + v.\nabla\right)T = k\nabla^2 T \qquad (18c)$$

where ρ, v, p and μ refers to density, velocity vector, pressure, dynamics viscosity, respectively. While c_p, k and T refer to heat capacity, thermal conductivity and temperature, respectively. The gravity term was not included as it has a negligible effect for the case of a horizontal HE.

3.4.2. CFD model. Figure 3.6 presents the schematic diagram of the horizontal EWHE. The CFD model is numerically solved using ANSYS Fluent 19.1 with a 3-D domain. Mesh independence study has been performed and a mesh of 7,987,446 elements has been deemed sufficient at a time step of 1 second in comparison to a mesh of 9,205,466 (Mesh 1) and 5,643,128 (Mesh 3) elements. The mesh shown in Figure 3.6: (a) Mesh Independence test. (b) and (c) Mesh constructed.

Figure 3.6 has been refined in the flow region where the highest gradients are expected and coarser in the soil region as convection is of a greater importance in comparison to conduction in this problem.

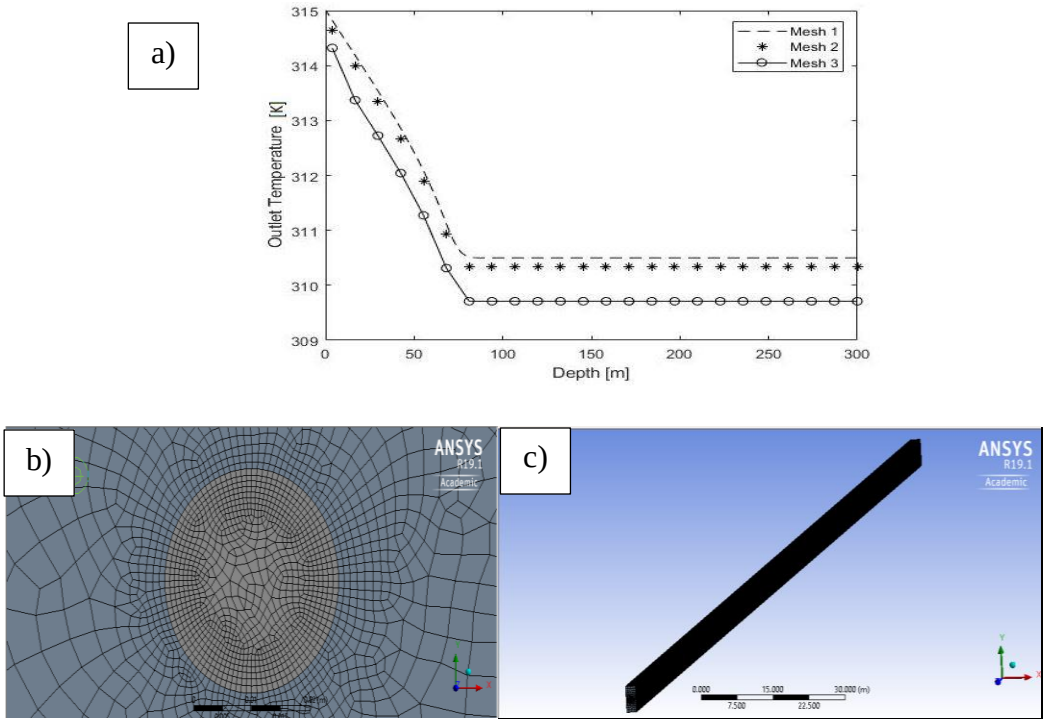

Figure 3.6: (a) Mesh Independence test. (b) and (c) Mesh constructed.

3.4.3. Turbulence model selection. Water is flowing in at a higher temperature than the ground temperature, thus the heat exchanger is in the cooling mode. The flow is incompressible, and the heat transfer is considered as conjugate heat transfer problem where is transferred from the water to the ground. For high Reynolds numbers and based on literature for flow inside a pipe, the realizable $k-\varepsilon$ model with enhanced wall treatment and thermal effects function option has been adopted in this [61].

$k-\varepsilon$ model is a two-equation model incorporating the Turbulence kinetic energy, equation (19), and the turbulence dissipation rate, equation (20) [103].

$$\frac{\partial k}{\partial t}+\mu_j\frac{\partial k}{\partial x_j}=\frac{\partial}{\partial x_j}\left[\frac{(v+v_{t)}}{\sigma_k}\frac{\partial k}{\partial x_j}\right]-\varepsilon+\tau_{ij}\frac{\partial \overline{u_\iota}}{\partial x_j} \tag{19}$$

$$\frac{\partial \varepsilon}{\partial t}+\mu_i\frac{\partial \varepsilon}{\partial x_j}=\frac{\partial}{\partial x_j}\left[\frac{(v+v_{t)}}{\sigma_\varepsilon}\frac{\partial \varepsilon}{\partial x_j}\right]+C_{\varepsilon 1}\frac{\varepsilon}{k}\tau_{ij}\frac{\partial \overline{u_\iota}}{\partial x_j}-C_{\varepsilon 2}\frac{\varepsilon^2}{k} \tag{20}$$

Where $v_t=C_\mu\frac{k^2}{\varepsilon}$, σ_k and σ_ε are the Prandtl number for k and ε, respectively. This model produces accurate results when studying turbulent shear flows but is inadequate in the presence of rotation or skewing. However, the modified model, realizable $k-\varepsilon$ model is considered to produce accurate results when predicting the flow in a wall-bounded and internal channels as C_μ is no longer a constant but is computed using an eddy-viscosity equation. The constants of the realizable the $k-\varepsilon$ model are $C_{\varepsilon 1}=1.44$, $C_{\varepsilon 2}$=1.9, σ_k=1.0 and σ_ε=1.2.

3.4.4. Specifications of the numerical study. As a solution method for this unsteady state problem, pressure-velocity coupling has been selected with a Semi-Implicit Method for Pressure Linked Equations (SIMPLE) algorithm. To model the thermal performance of the horizontal ground heat exchanger as a function of time the boundary conditions applied matched the actual conditions obtained from the experimental setup. Temperature defined at the upper and lower surface for depth (z) are as follows, at z= 0 m, T= 318 K and at z=4 m, T=303 K, the sides are set as adiabatic with a heat flux equal to zero. The inlet mass flow rate is varied between 0.15, 0.075 and 0.0375 kg/s. Two cases have been studied by varying the inlet temperature from 315 K to 340 K. The simulation conditions used in this work are reported in The performance of the heat exchanger over a certain period is evaluated by studying the

heat passing through the pipes to the ground. The soil properties are set as homogenous and maintained constant throughout the simulation.

Table 3.2. The performance of the heat exchanger over a certain period is evaluated by studying the heat passing through the pipes to the ground. The soil properties are set as homogenous and maintained constant throughout the simulation.

Table 3.2: Simulation Conditions.

Parameter	**Value**
Diameter of EWHE (m)	0.03
Length of EWHE (m)	300/100
Trench depth (m)	2.5
Density of soil ($kg.m^{-3}$)	1400
Thermal conductivity of soil ($W.m^{-}1.K^{-1}$)	1.4
Specific heat of soil ($J.kg^{-1}.K^{-1}$)	856
Density of circulation fluid inside pipe ($kg.m^{-3}$)	998.2
Temperature of fluid (K)	340/ 315
Fluid flow velocity (m/s)	0.2123
Specific heat of circulation fluid ($J.kg^{-1}.K^{-1}$)	4183
Thermal conductivity of water ($W.m^{-}1.K^{-1}$)	0.6
Dynamic viscosity of water ($kg.m^{-1}.s^{-1}$)	0.001

3.5. Parametric Study

A 3-D steady state domain is developed to examine the effect of inlet water temperature, water velocity, soil thermal conductivity and ground surface temperature on the rate of heat transfer using ANSYS FLUENT 19.1. The Boundary conditions adopted are outlined in Table 3.3. The boundary conditions for the wall separating the

water domain and the sand domain are set as coupled wall. This will solve the Navier-Stokes equations in the fluid zone and the heat conduction equations in the solid zone, known as conjugate heat transfer.

Table 3.3: Boundary conditions.

Parameter	Value
Upper surface temperature (K)	318
Inlet water temperature (K)	340
Inlet water velocity (m/s)	0.2123
Outlet water pressure (kPa)	0

The model produced for the transient study was utilized for the steady state parametric analysis. A time step of 1 second was chosen and 300 iterations for each run. The convergence criteria for each of the parameters was maintained as default and the boundary conditions where varied sequentially. The dimensions of the model were maintained as in the transient case. The total height of the sand at four meters, a width of one meter at each side of the pipe and a pipe diameter of three cm. The heat transfer around a pipe generally doesn't extend beyond twenty times the pipe diameter. Thus, by maintaining a sand thickness of 1 meter at each side the adiabatic boundary conditions set at the side walls can be justified. It is established from literature that the pipe material imposes a negligible effect on the rate of heat transfer and thus was not considered in this study.

Chapter 4. Results and Discussion

In this study, the rate of heat rejected to the ground and thus the ground cooling potential is analyzed. This chapter offers better understanding of EWHE by reporting and discussing experimental and numerical results of multiple tests.

This chapter is divided to four sections, mainly (1) soil analysis, (2) borehole underground temperature, (3) Results for 300 meters underground EWHE and (4) numerical simulation.

4.1. Soil Analysis

4.1.1. Soil composition. The performance of the heat exchanger varies based on the soil properties which are dictated by the soil composition. Figure 4.1 (A) shows the elemental analysis obtained using an energy dispersive X-ray spectroscopy (EDS). The EDS analysis shows the distribution of the elements with a dominance of calcium, silicon with carbon and oxygen having a combined weight percent of 80%. XRD analysis was executed and the sample exhibited the expected domination of quartz (SiO_2 at 51.4%) and calcite ($CaCO_3$ at 35.2%).

The rest of the sample consisted of albite ($Na_{0.75}Ca_{0.25}$) $Al_{1.26}Si_{2.74}O_8$ at 10% and traces of dolomite (CaMg (CO_3) at 3.4%). The last two compounds are an oxide and a carbonate, and both possess a high degree of stability, with minimal effects on the weight of the sand. Figure 4.1 (B) shows the elements distribution using EDS mapping with (a) Oxygen, (b) Calcium, (c) Silicon and (d) Carbon.

As for the size distribution of the particles within the sample, a built-in image analysis software in SEM produced the histogram of Figure 4.2 showing the dominance of particles less than 2 µm in size, while other significant sizes appear between the 120-220 µm band.

Figure 4.2 shows the size distribution of the particles within the sample, a built-in image analysis software in SEM produced the histogram showing the dominance of particles less than 2 µm in size, while other significant sizes appear between the 120-220 µm band. The small size of the particles results in ease of compaction. The effect of compaction on soil thermal properties is discussed in section 4.1.2.

(A)

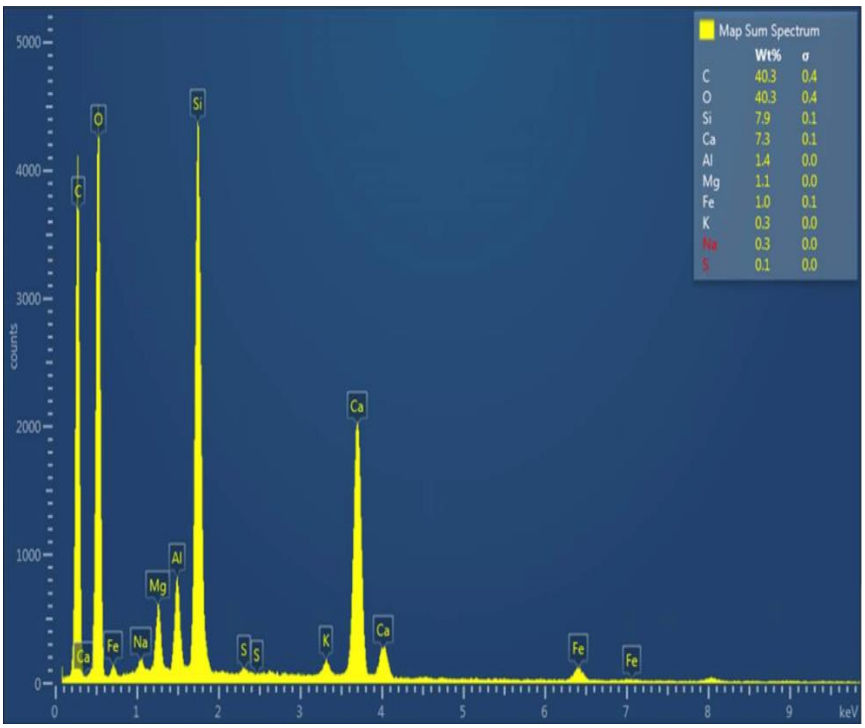

(B)

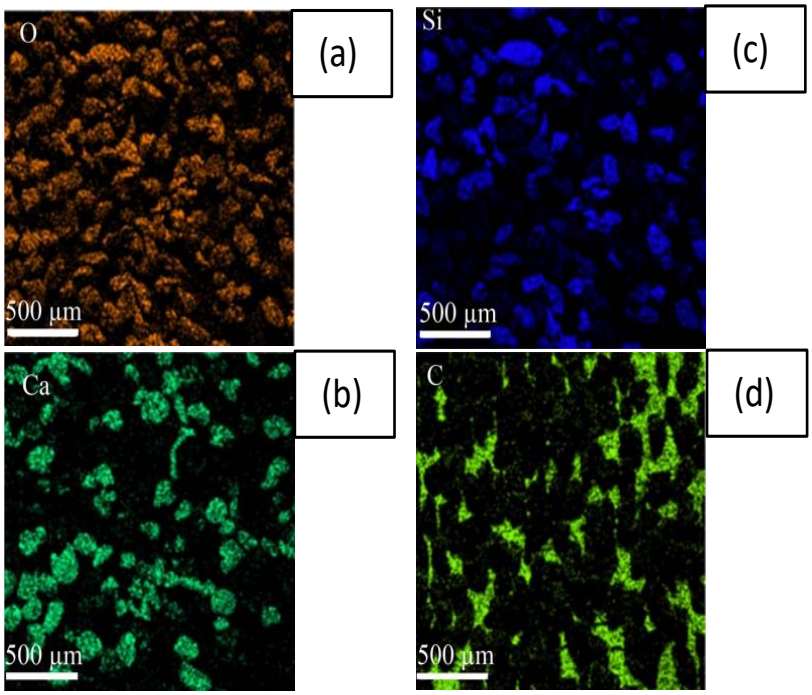

Figure 4.1: (A) EDS elemental analysis of soil sample and (B) EDS mapping of the main elements(a) Oxygen, (b) Calcium, (c) Silicon and (d) Carbon.

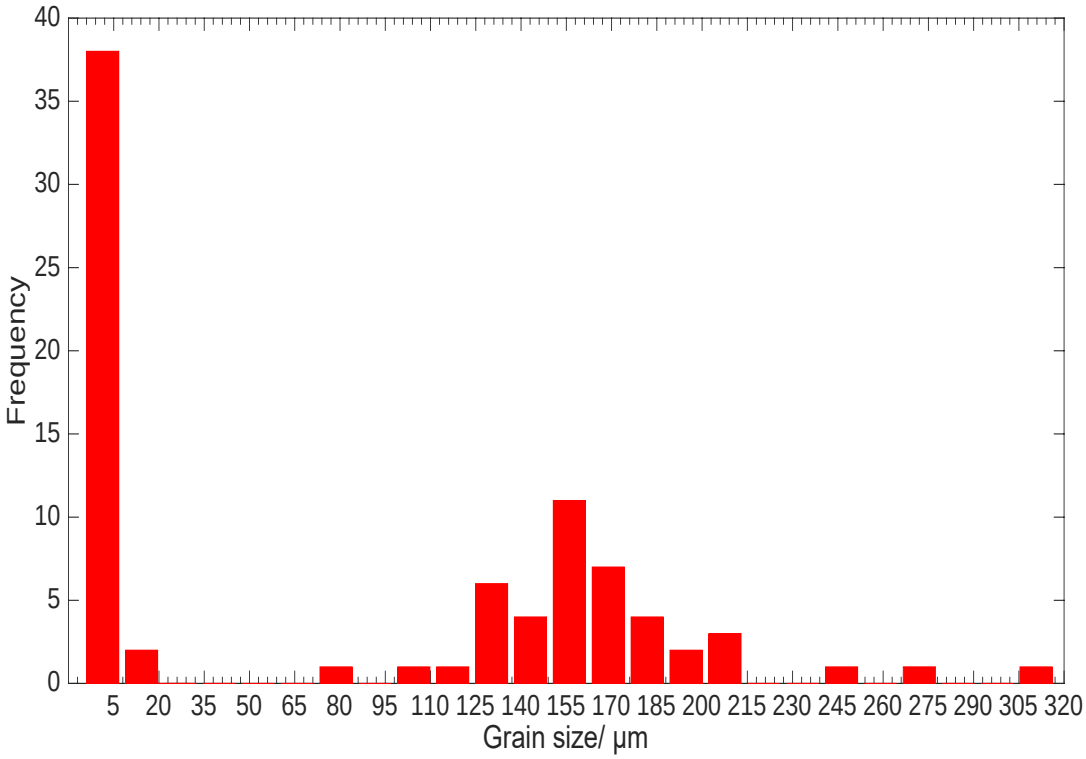

Figure 4.2: Particle size distribution based on SEM images.

4.1.2. Soil thermal analysis. In general, sand particle size, water content, saturation level, and soil compaction influence the thermal conductivity of soil. Analyzing the thermal conductivity of soil as a function of the previously mentioned parameters is necessary to understand the flow of heat around earth-to-water heat exchanger. Samples were collected at depth of 2 m below ground level from an area located within the American university of Sharjah Campus. The thermal conductivity of these samples was measured using thermal conductivity analyzer from C-Therm Technologies.

The effect of water content on the thermal conductivity is shown in Figure 4.3(a) where a direct relation was obtained between water content and conductivity. That was expected given that water has a thermal conductivity of 0.613 W/m.K in contrast to the low conductivity of air at 0.028 W/m.K. The opposite trend was observed between porosity and thermal conductivity. Higher porosity exists at lower compaction levels, thus more air in the sample. This explains the inverse relation however; this effect is dominant at low water content levels as shown by the steep curve at two percent water content in Figure 4.3.

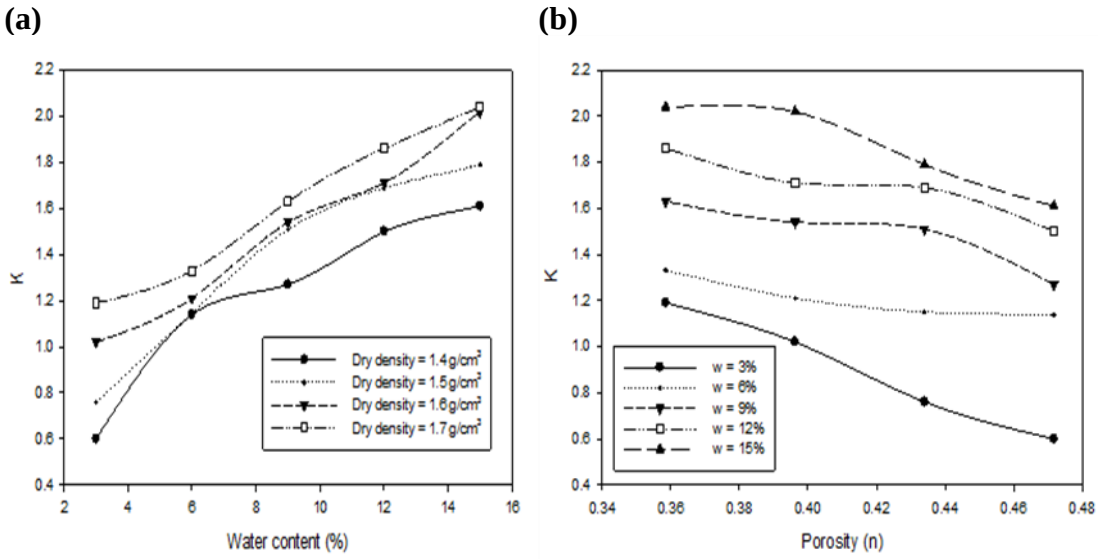

Figure 4.3. Effect of (a) water content (b) porosity on soil thermal conductivity.

Analyzing the data obtained experimentally, it was observed that an increase in water content has a greater impact on thermal conductivity of sand than initial dry density. The thermal conductivity increased from 39% to 63% when the water content was increased from 3% to 15% under different compaction levels.

4.2. Temperature Distribution

The depth at which the heat exchanger is placed influences the rate of heat exchange due to the variation in soil temperature. C. O. Popiel et al. distinguished three ground zones into: Surface zone reaching a depth of about 1m, shallow zone extending from the depth of about 1 to 8 m (for dry light soils) or 20 m (for moist heavy sandy soils) and deep zone below the depth of the shallow zone [104].

4.2.1. Ground temperature distribution obtained mathematically. A mathematical model based on the air temperature and soil diffusivity was developed by Kasuda [105] to predict ground temperature distribution as shown in equation (24).

$$T_{soil(D,tyear)} = T_{mean} - T_{amp} e^{\left(-D\sqrt{\frac{\pi}{365*\alpha}}\right)} \cos\left(\frac{2\pi}{365}\left(t_{year} - t_{shift} - \frac{D}{2}\sqrt{\frac{365}{\pi\alpha}}\right)\right) \quad (24)$$

Where T_{mean} is mean ground temperature (average air temperature), also known as the undisturbed temperature. T_{amp} is amplitude of surface temperature which is calculated as $T_{amplitude} = (T_{max} - T_{min})/2D$ where T_{max} is the maximum air

temperature, T_{min} is the minimum air temperature and D is the depth below surface in meters. α is thermal diffusivity of soil, t_{year} the current time (in days) and t_{shift} refers to the day of the year at which the minimum surface temperature occurs.

Utilizing the Kasuda model [105] and based on weather data in Sharjah obtained from the National Centre of Meteorology and Seismology in UAE, the ground temperature for each month has been calculated as shown in Figure 4.4. As shown in the figure. The temperature at the surface is higher than underground temperature during the summer which facilitates cooling. The opposite trend is observed in the winter where the temperature below the ground is higher than ground surface temperature which facilitates a heating potential. The temperature is assumed to reach a constant value known as the undisturbed temperature at a depth of 12 m [32]. The undisturbed temperature based on this model is around 27°C and is equal to the average ambient air temperature.

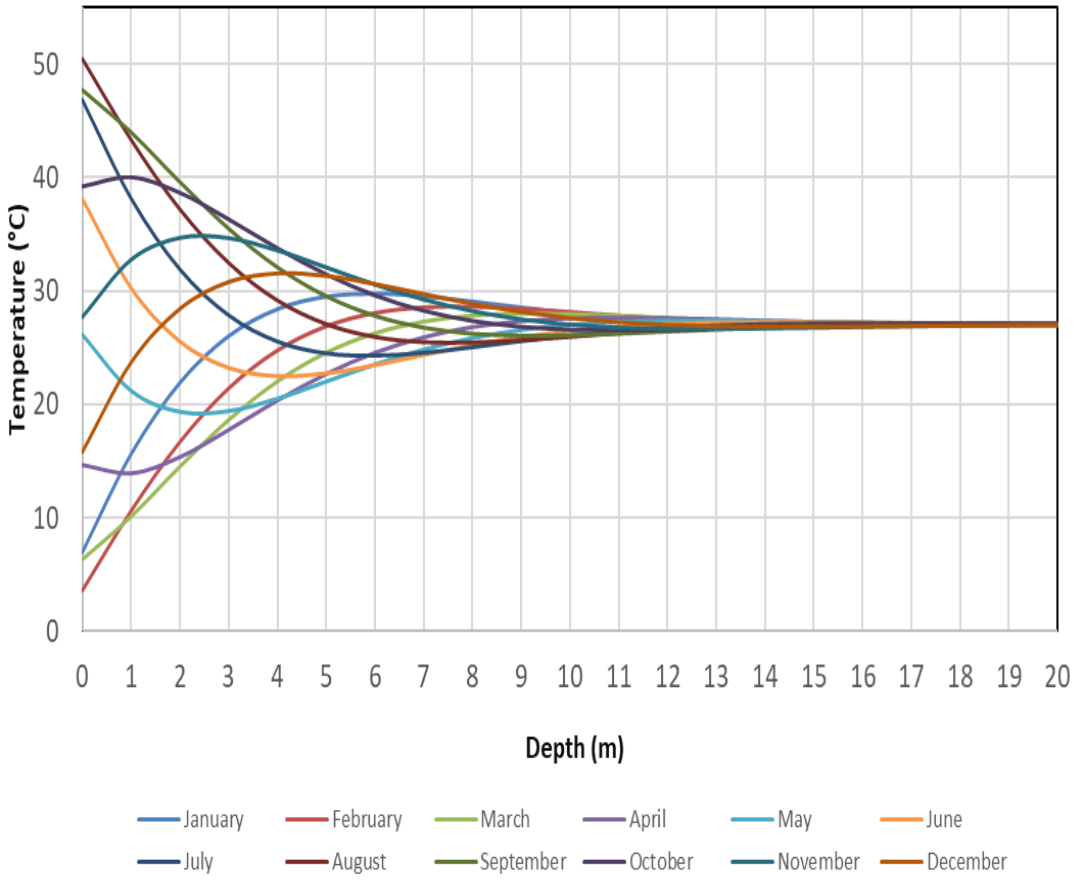

Figure 4.4: Ground vertical temperature distribution based on Kasuda.

The above model relies on the accuracy of the input variables and assumes the ground surface temperature to equal the air temperature, which is a very rough assumption. To predict the performance of the heat exchanger accurately, the precise ground temperature is required due to its significant influence. To obtain reliable data an experimental setup has been constructed to measure the ground temperature distribution at two locations in Sharjah as discussed in 4.2.2.

4.2.2. Ground temperature obtained from two boreholes in Sharjah. Given that the type of ground surrounding boreholes may affect the ground temperature, two experimental location have been constructed. The first location indicated as borehole one (BH1) which is located in a shaded area near a tree and irrigated zone. The second borehole (BH2) referred to as borehole two which is located in a non-shaded sandy area with bare ground surface.

Temperature readings have been recorded hourly using seven K-Type thermocouples for each borehole. Monthly average ground temperature measurements for the period between March to September over the entire depth have shown that the annual temperature cycle had penetrated to a depth of 8 m as shown in Figure 4.5 and Figure 4.6. Considering BH1, measurements have shown that the ground temperature increases for a depth of 2 m. This means that heat was transferred up to the ground surface. While from June to September the ground temperature decreases with depth. Which indicates that heat flux was transferred from the surface to the shallow zone of the ground.

Therefore, the surface zone in the UAE at which the ground is exhibits high response to change in short time weather conditions lies within the first two meters. The shallow zone at which the temperature varies seasonally can be estimated to be between 2 to 8 m. The deep zone at which the temperature is generally constant exists at a depth below 8 m.

Furthermore, over the study period, the fluctuation in the amplitude of the surface temperature at borehole one is less than that at borehole 2. With a surface temperature range of 24.69 to 37.7°C and 23 to 40.7°Cat borehole 1 and 2, respectively. Thus, placing the heat exchanger in a shaded area will aid in reducing the climatic influence on the thermal performance for shallow heat exchangers.

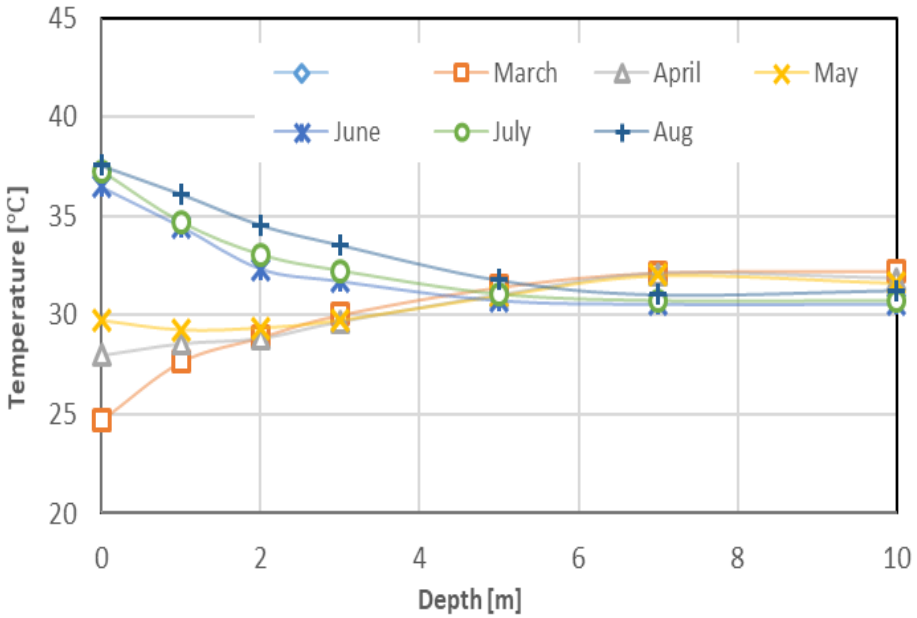

Figure 4.5: Ground Temperature Distribution at Borehole 1.

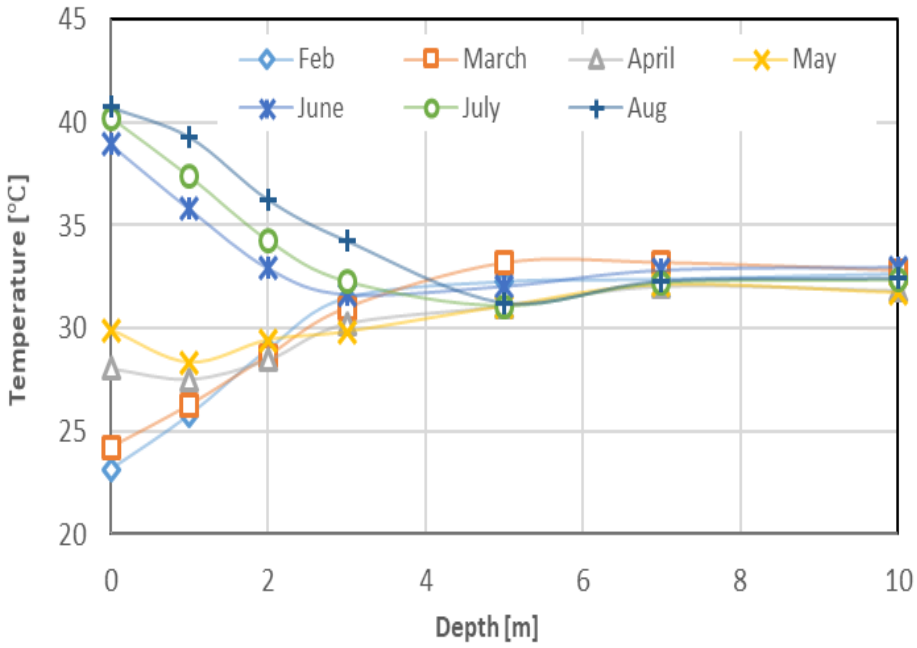

Figure 4.6: Ground Temperature Distribution at Borehole 2.

The ground temperature distribution during June, July, and August as a function of depth as recorded for both boreholes is presented in Figure 4.7, Figure 4.8, and Figure 4.9. The variation in temperature based on surface type was noticeable in the first few meters with a 3~4°C difference at the surface and it diminishes with depth. The surface

temperature difference between borehole one and two was at its minimum in June and increased towards august. That's because the solar radiation intensity increased to reach its peak and its impact became significant. That explains why the temperatures at both boreholes coincide at two meters in June, three meters in July and at four meters in August.

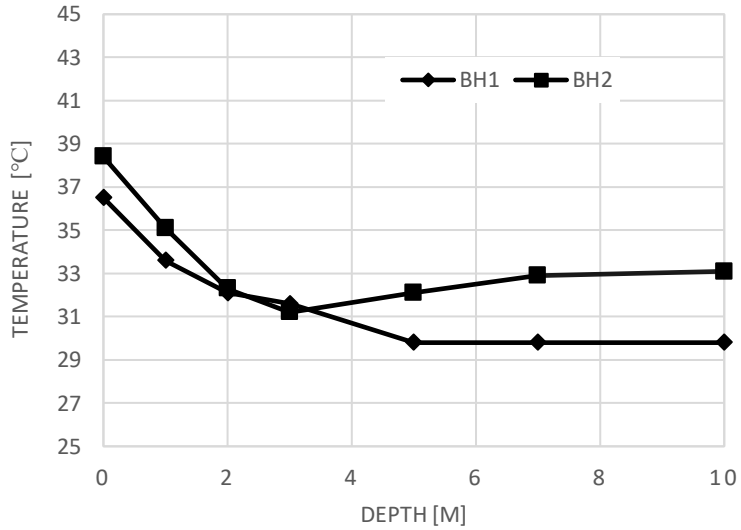

Figure 4.7: Ground temperature distribution in June.

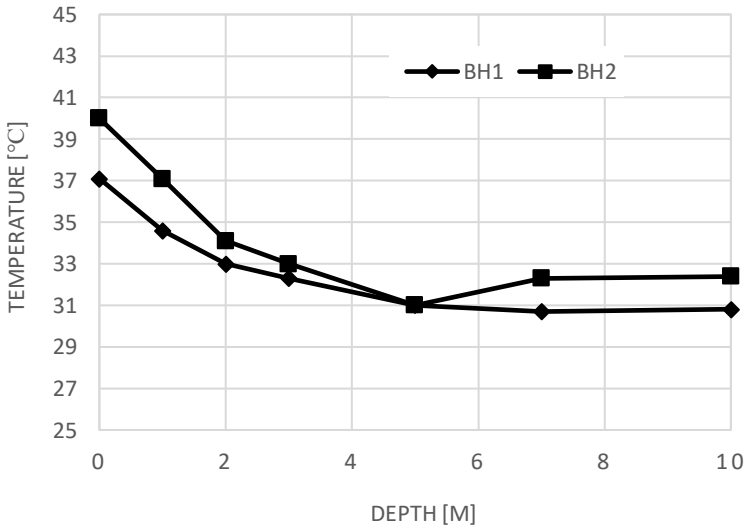

Figure 4.8: Ground temperature distribution in July.

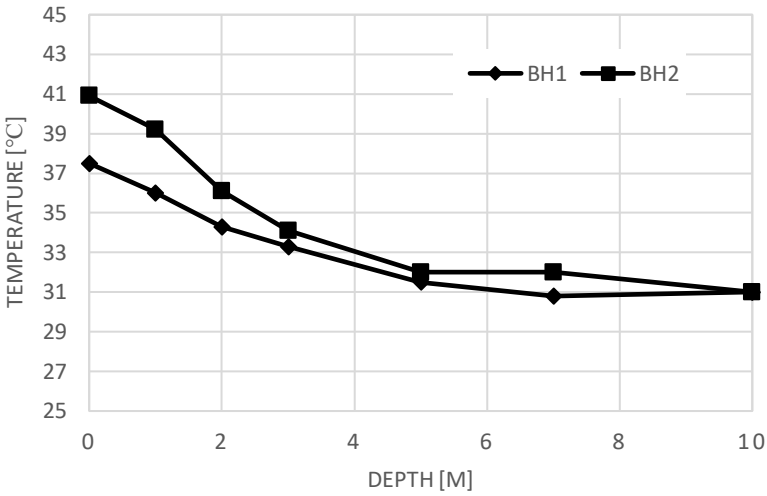

Figure 4.9: Ground temperature distribution in August.

Figure 4.10 compares the temperature distribution predicted using Kasuda model to the one measured in both boreholes. The figure shows the results for the two months, namely March and September. The figure shows that Kasuda model underestimates the surface temperature in March and overestimates the ground temperature in September.

Furthermore, Kasuda model underestimate the undisturbed temperature by around 5°C. However, Kasuda model is able to predict the point where temperature start to stabilize which occurs at a depth of 7~8 m. The Kasuda model underestimate the undisturbed ground temperature since Kasuda model assumes that the undisturbed temperature is year-average ambient temperature.

This assumption is not very realistic, and this can be seen in Figure 4.11 which displays the variation of ground temperature at each depth in relation to ambient temperature on the 6th of August. At night the ambient air temperature is lower than that of the surface. During daytime the ambient air temperature is higher than that of the surface. As shown in the figure a maximum difference of 10.1°C was observed at 10:19:54 AM and a minimum of 0.1°C at 4:19:00 PM. Furthermore, a 12 hours phase delay is noticed between the ambient air temperature and the ground temperature with peak ambient temperature at after 22 hours followed by a peak in ground temperature at 34 hours.

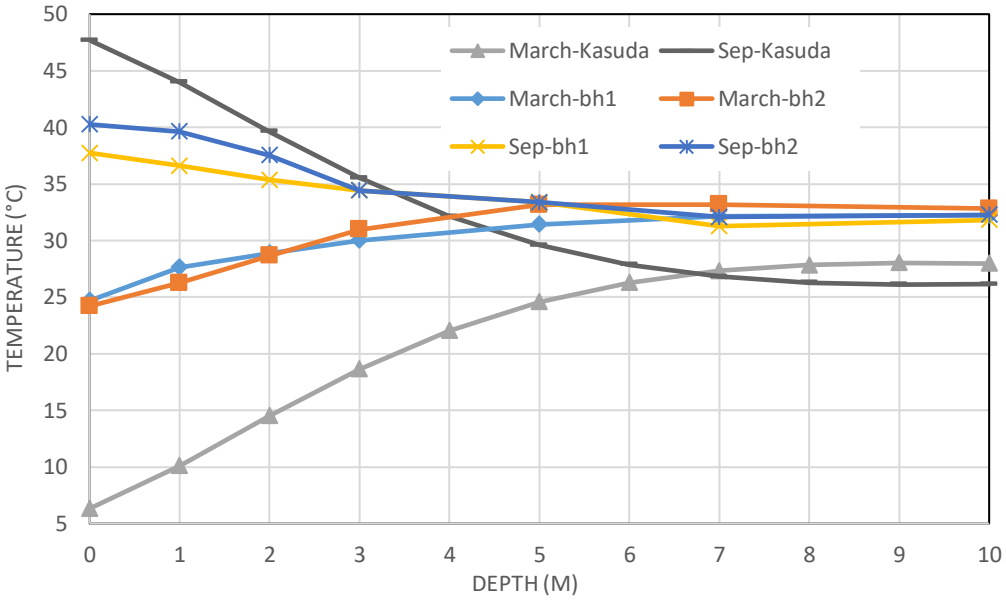

Figure 4.10: Comparison of Temperature Distribution obtained using Kasuda to measurements for the months of March and September.

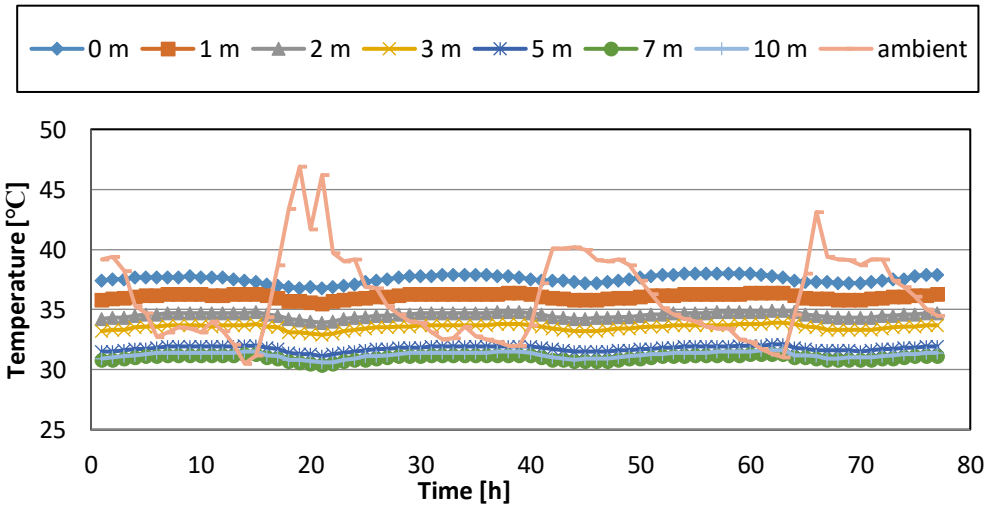

Figure 4.11: Ambient air and ground temperature on the 6th of August.

4.3. Trench Setup Results and Analysis

4.3.1. EWHE performance with inlet temperature of 315 K. To investigate the heat exchange rate for three mass flow rates, the setup explained earlier was utilized. Temperature sensors fixed at the inlet and the outlet of the GHE were used to measure the water temperature which was recorded by a data logger at a time interval of one

minute in addition to the ambient air temperature. The heat exchange rate was calculated using the below equation (25).

$$\dot{Q} = \dot{m} c_p \Delta T \tag{25}$$

Where $\dot{m}$ is the mass flow rate of the system, c_p refers to the specific heat capacity of the fluid and $\Delta T = T_{in} - T_{out}$ for cooling.

A positive ΔT in this case indicates that the EWHE was operating in the cooling mode, thus heat was rejected to the ground. Temperatures recoded and heat exchange rate calculated are shown in Figure 4.12, Figure 4.13, and Figure 4.14 for mass flow rates of 0.15, 0.075 and 0.0375 kg/s, respectively. The heat exchange rate is high initially at 3.135 kW due to the major difference in temperature between the flow and the ground. However, after some time ground temperature increases, decreasing the rate of heat exchanged. This continues until a state of ground retention is reached at which the ground is saturated near the pipe and can no longer absorb heat. This can be avoided by adopting intermittent operation instead of continuous flow. The advantage of burying the condenser underground is obvious with the ambient air temperature about 10°C higher than that of the ground.

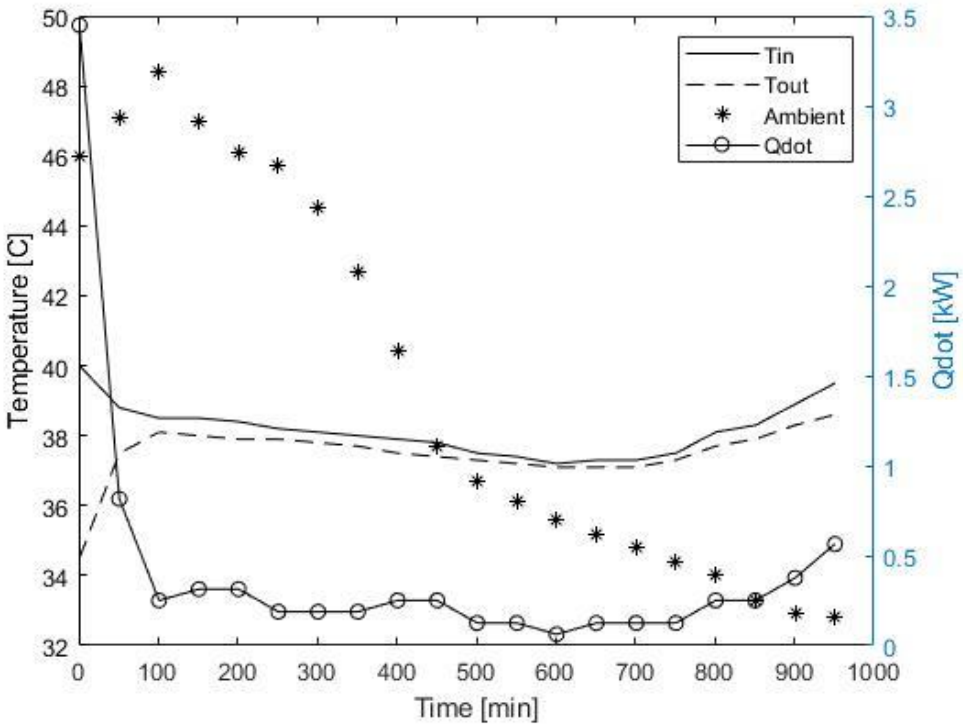

Figure 4.12: Results at inlet temperature of 315 K and flow rate of 0.15 kg/s.

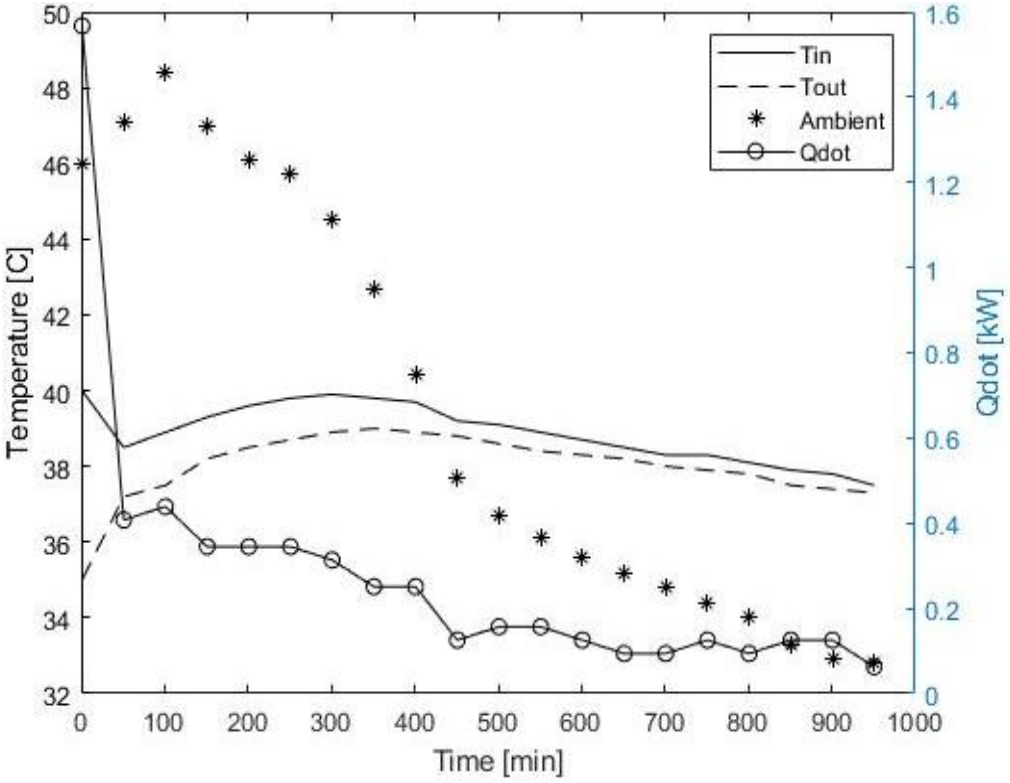

Figure 4.13: Results at inlet temperature of 315 K and flow rate of 0.075 kg/s.

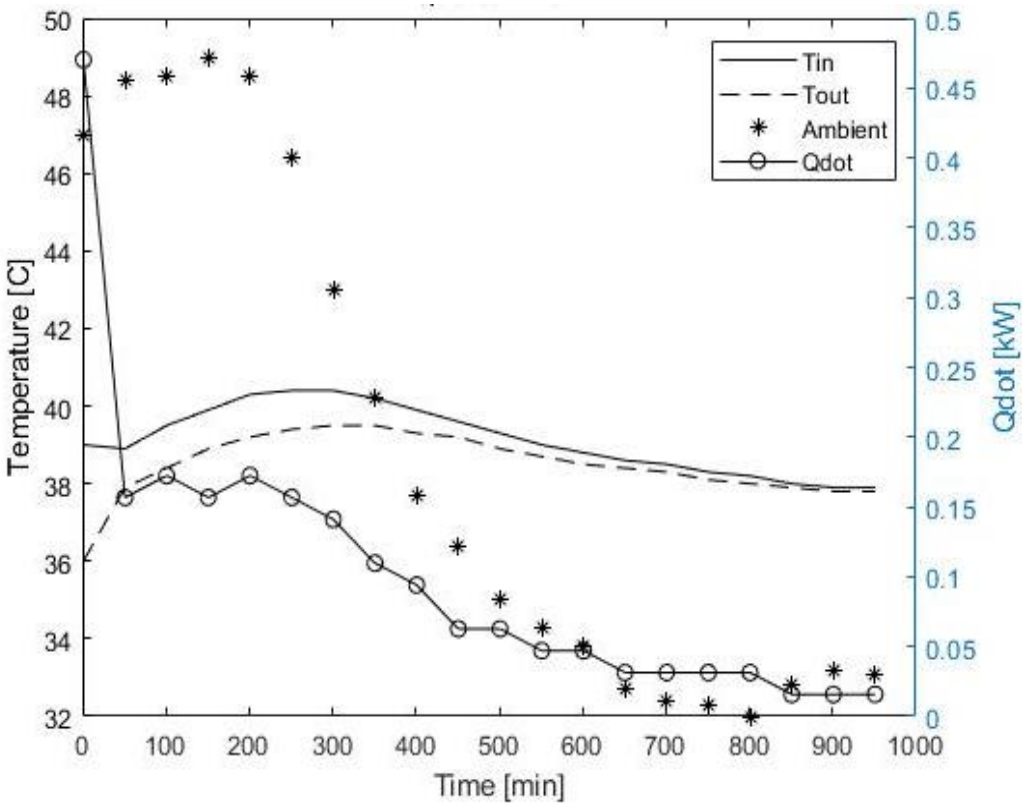

Figure 4.14: Results at inlet temperature of 315 K and flow rate of 0.0375 kg/s.

Effectiveness is commonly used to evaluate the performance of a heat exchanger. It is the ratio between the actual heat extracted or rejected to the maximum heat transfer. The actual heat rejected maybe calculated as stated in equation (26) while the maximum heat transfer was calculated as shown in equation (27).

$$\dot{Q}_{max} = \dot{m}_{water} c_{p,water} \left(T_{in} - T_{ground}\right) \tag{26}$$

Which simplifies to

$$\varepsilon = \frac{T_{in} - T_{out}}{T_{in} - T_{ground}} \tag{27}$$

Figure 4.15 shows the effectiveness of the heat exchanger at full flow, half flow and quarter the initial flow rate, respectively. It can be seen that the effectiveness is at its maximum at the beginning of the operation. However, it decreases with time and reaches a zero when the water is no longer being cooled by earth. The time taken for the effectiveness to reach the minimum was shortest in the case of the maximum flow rate and longest at the minimum flow rate.

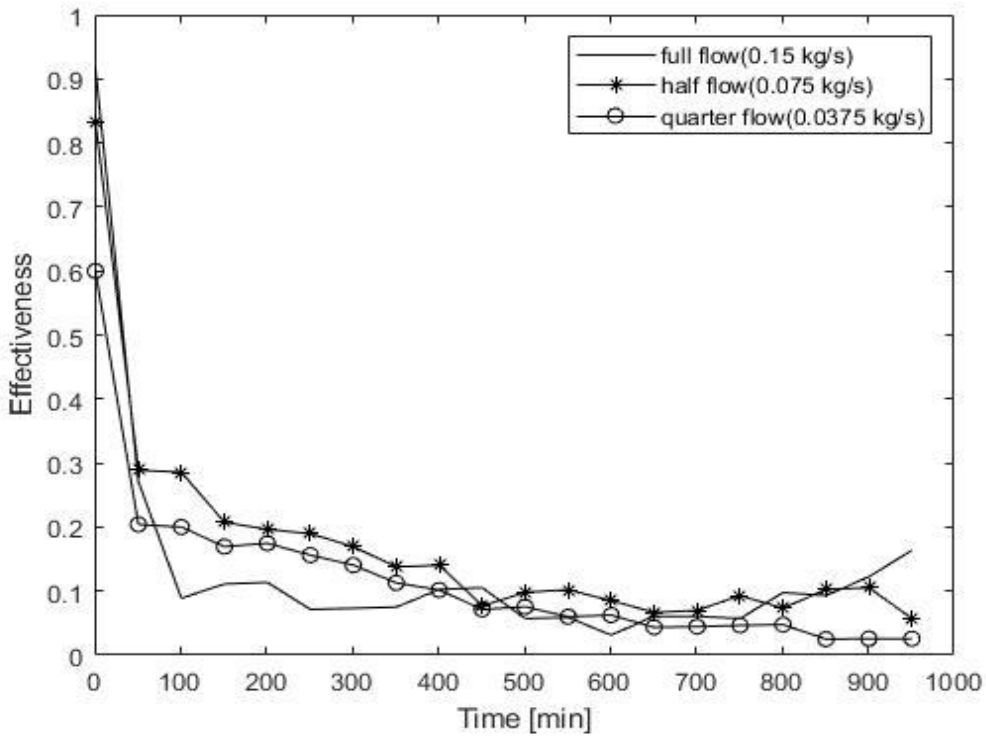

Figure 4.15: Heat Exchanger Effectiveness at full, half and quarter flow rate.

4.3.2. EWHE performance with inlet temperature of 340 K. The minimum temperature the inlet water can cool to is equal to the ground temperature at which the GHE is located. Thus, a higher inlet temperature will result in a higher rate of heat exchanged. To study this effect experimentally, a water heater of 100 L capacity was connected to the water tanks. Thus, given the experimental limitation the potential of the ground to absorb heat was only studied while the supply of hot water lasted.

To prolong the period of heat exchange between the ground and water entering at 340 K, the mass flow rate was decreased to half and quarter the full mass flow rate using a control valve. For each run, the water inlet, outlet and ambient air temperatures were recorded. Using the experimental data, the rate of heat exchanged and the effectiveness of the ground heat exchanger at each mass flow rate were calculated. Figure 4.16, Figure 4.18, and Figure 4.18 show the recorded temperatures and the calculated rate of heat exchange at full, half and quarter the mass flow rate respectively.

The full flow rate exhibited the highest rate of heat exchange with a maximum value of 19.1 kW initially. The rate decreased with time as the inlet temperature was decreasing and thus no conclusion about the ground saturation could be reached from this run. However, it can be concluded that the potential for cooling is greater with elevated inlet temperatures as the maximum change in temperature for this case was 30°C in comparison to 5°C at an inlet temperature of 15 K.

The effectiveness for each case was calculated and plotted over time as shown in Figure 4.17, Figure 4.19 and Figure 4.21. Decreasing the mass flow rate to quarter extended the time before effectiveness reaches zero, from 22 minutes at full flow to about 35 minutes at quarter the flow. After that, the direction of heat exchange is reversed as the water supplied by the heater is circulated and the water in the tank which is at 315 K begins to flow.

At that point the ground has been heated up by the supply from the heater and thus, is at a greater temperature than that of the tank water. Resulting in heat rejection to the flow. Producing a negative effectiveness when calculated using the equation designed for the cooling mode.

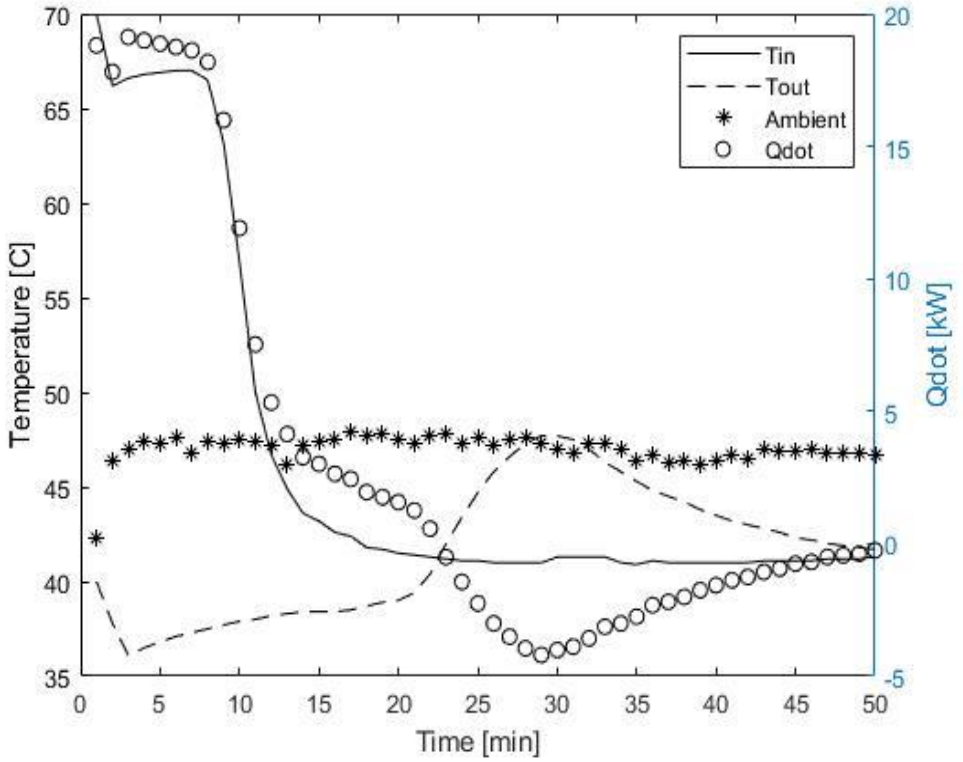

Figure 4.16: Results at inlet temperature of 340 K and flow rate of 0.15 kg/s.

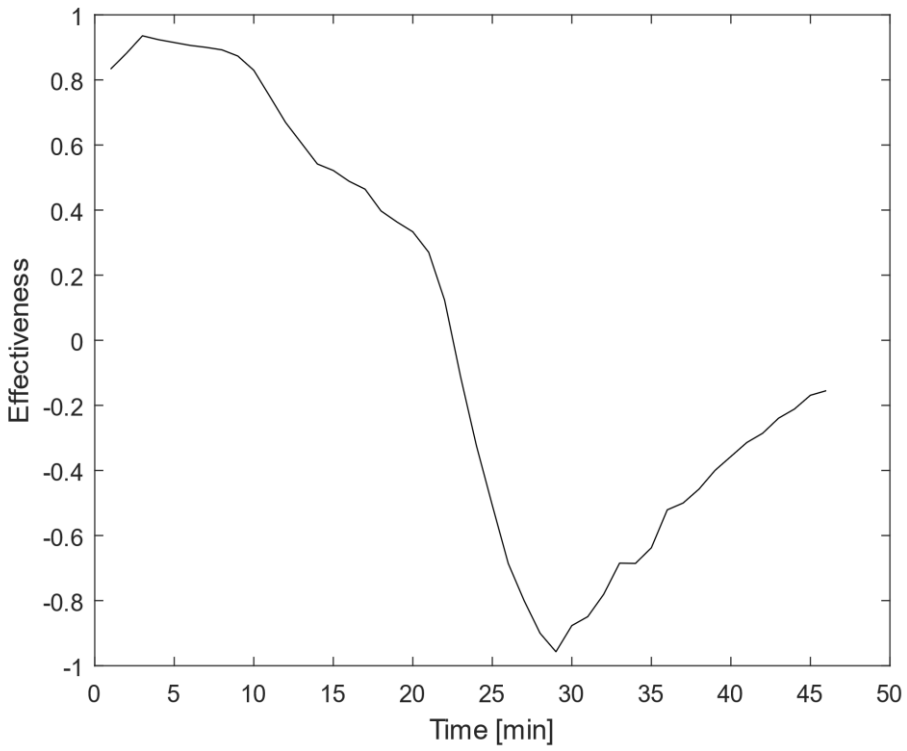

Figure 4.17: Heat Exchanger Effectiveness at a flow rate of 0.0375 kg/s.

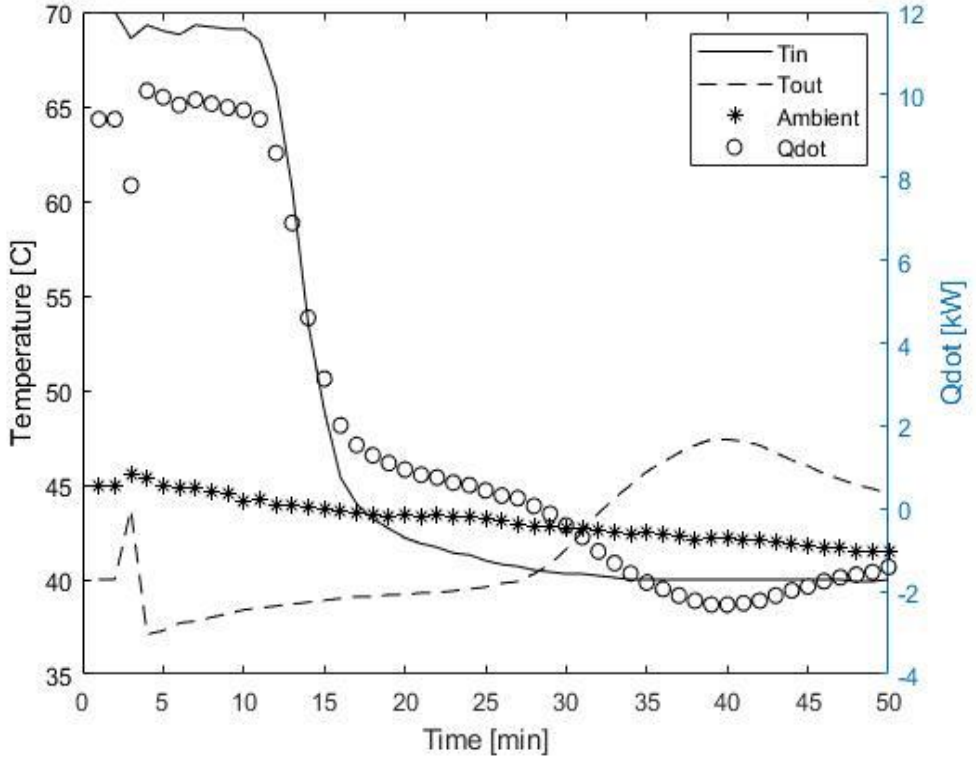

Figure 4.18: Results at inlet temperature of 340 K and flow rate of 0.075 kg/s.

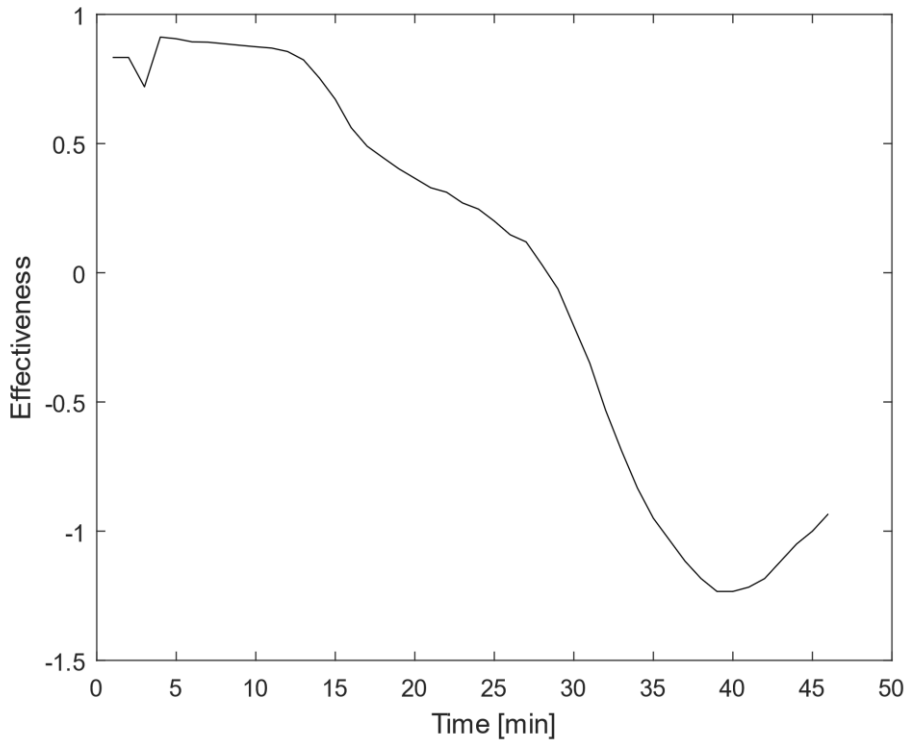

Figure 4.19: Heat Exchanger Effectiveness at a flow rate of 0.075 kg/s.

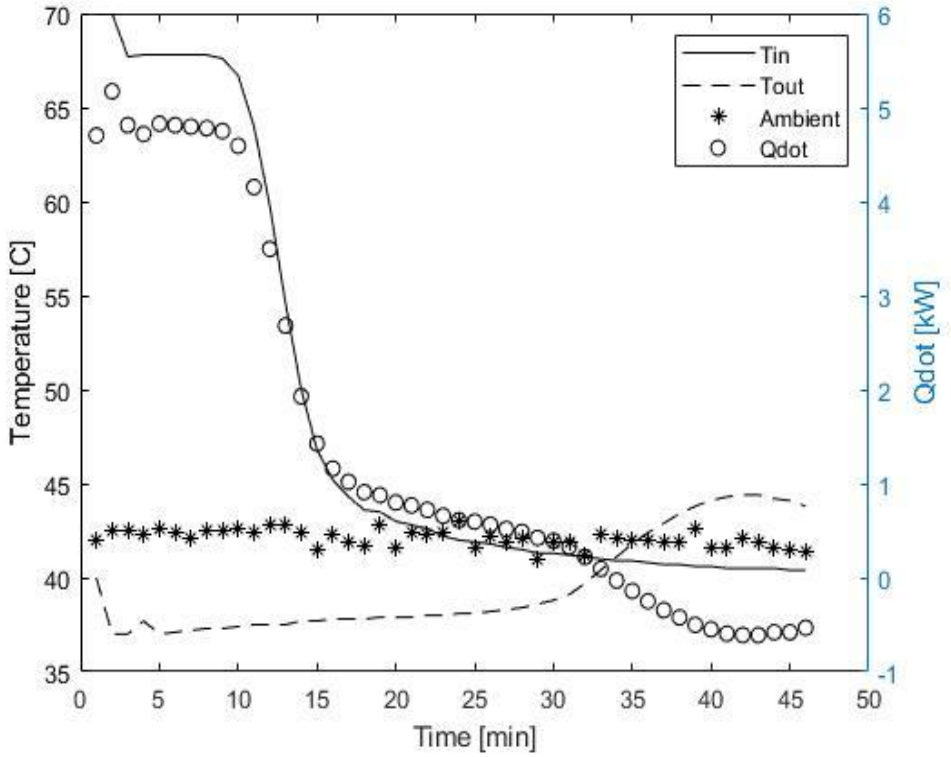

Figure 4.20: Results at inlet temperature of 340 K and flow rate of 0.0375 kg/s.

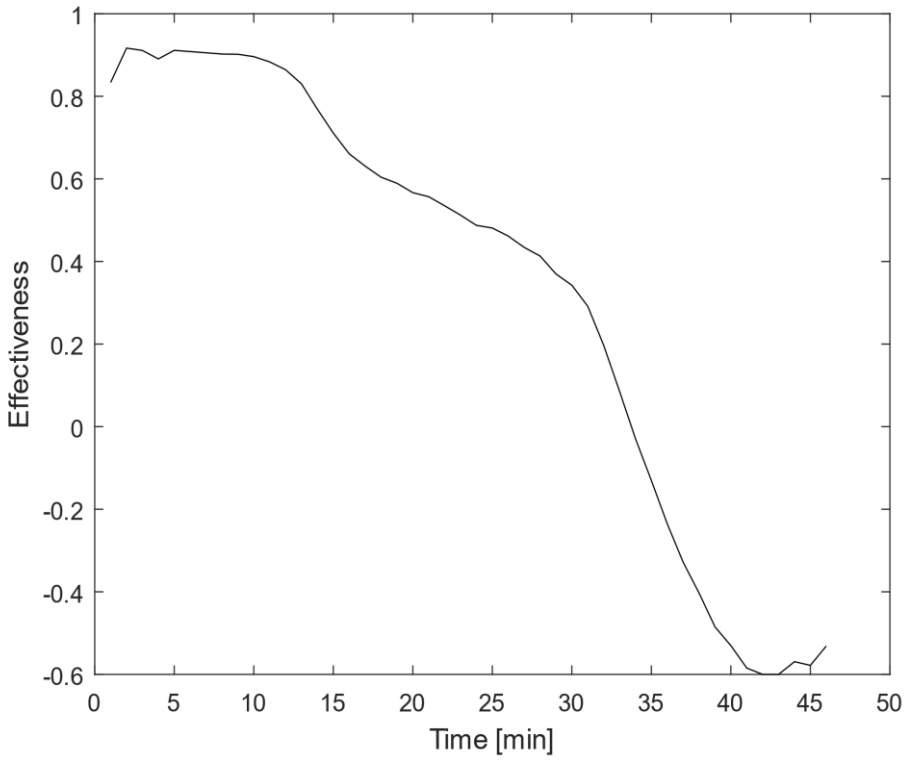

Figure 4.21: Heat Exchanger Effectiveness at a flow rate of 0.0375 kg/s.

4.4. Transient 3D Numerical Simulation

The CFD simulation has been used to study the performance of the EWHE at different operating inlet temperatures. Considering the actual weather conditions in the UAE, the soil properties obtained, and the setup mentioned earlier in chapter 3, a numerical model was developed. ANSYS Fluent 19.1 is used to study different scenarios and time periods while mimicking the experimental case. Figure 4.22 reports the water outlet temperature over the pipe length for a water inlet temperature of 340 K. The four lines represent the operation at time of 300, 800, 1000, and 1500 s. As expected, for the same length or more precisely at the same position, longer operation time degrades the performance of the heat exchanger. Figure 4.23 reports the water outlet temperature over the pipe length for a water inlet temperature of 315 K. The length required for cooling to the minimum temperature increases with increasing running time. That is clearly indicated by the drop-in effectiveness value calculated at a length of 60 meters over time as shown in Figure 4.24. The effectiveness was high initially but decreased with time, this is attributed to the increase in soil temperature.

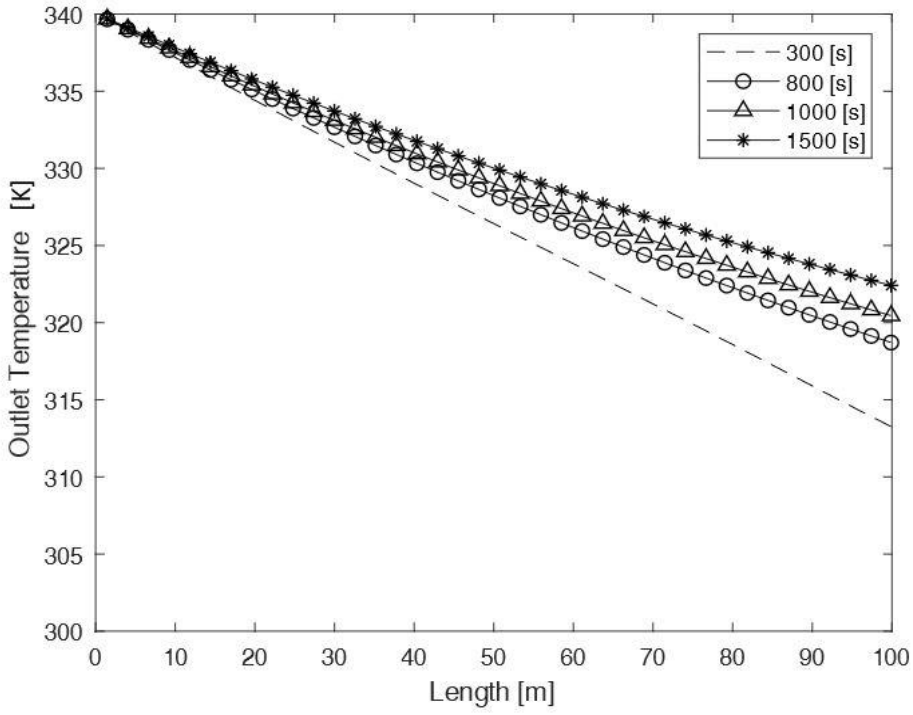

Figure 4.22: Outlet temperature over length at various running times with inlet velocity of 0.2123 m/s and inlet temperature of 340 K.

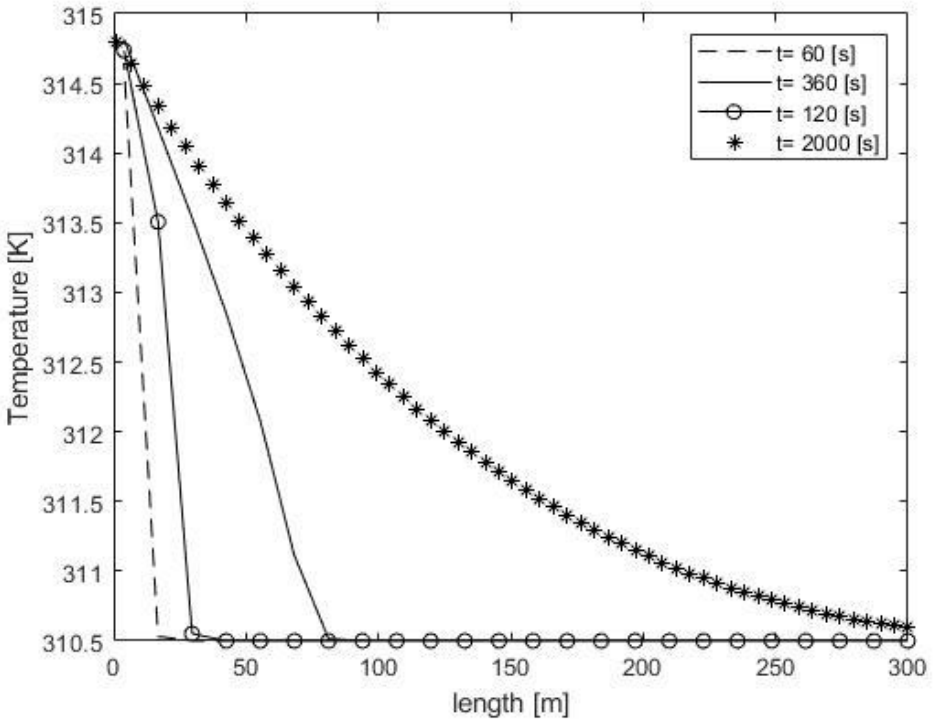

Figure 4.23: Outlet temperature over length at various running times with inlet velocity of 0.2123 m/s and inlet temperature of 315 K.

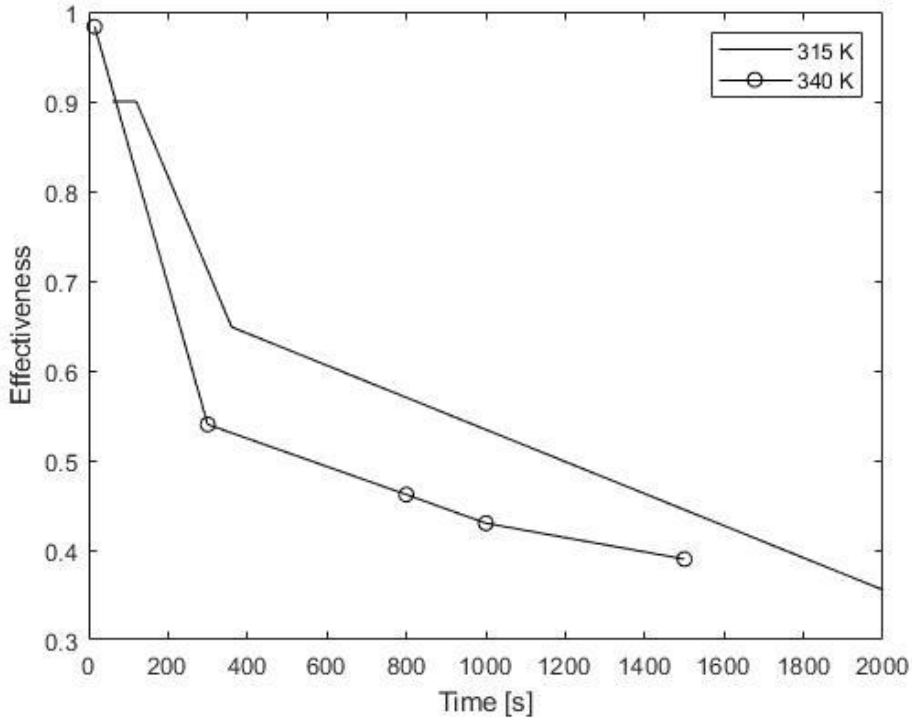

Figure 4.24: Effectiveness at different inlet temperatures at a flow rate 0f 0.15 kg/s.

4.5. Parametric Steady State 3D Numerical Simulation

4.5.1. Effect of soil thermal conductivity. Several studies in literature reported soil thermal conductivity values ranging between 1 W/m.K with values up to 3 W/m.K [106]. It is influenced by the water content, saturation degree, temperature and mineral composition [2]. To evaluate the effect of varying soil thermal conductivity, all other parameters including fluid velocity, inlet temperature and ground surface temperature are kept constant. In Figure 4.25, the effect of soil thermal conductivity on water outlet temperature is presented. It was observed that as soil thermal conductivity increases, the amount of heat transfer from the pipe to the soil increases, hence water outlet temperature decreases. The increase in rate of heat exchange is proportional to the increase in soil thermal conductivity. This is deduced from the decreasing outlet temperature at higher soil thermal conductivities. Thus, it is critical to test the soil thermal conductivity prior to the installation of a ground heat exchanger since this will dramatically dictate the size and length of an EWHE. A soil thermal conductivity of 3 W/m.K resulted in a temperature drop greater than 10°C. In general, sizing the EWHE will depend on the application requirements.

4.5.2. Effect of fluid velocity. In Figure 4.26, the effect of fluid velocity on water temperature is shown. Water outlet temperature increases with an increase in fluid velocity. A higher velocity results in a greater mass flow rate. An inverse relation was observed between the mass flow rate and ΔT for a constant rate of heat transfer. It is expected that as the velocity increases the Reynolds number increases, but the time of contact between the fluid and the ground is reduced. For cooling applications, a higher ΔT is desired. Thus, a compromise is to be made between flow rate and residence time to optimize heat transfer.

4.5.3. Effect of fluid inlet temperature. It is established that a high temperature difference between the inlet fluid and the outlet fluid indicates an enhanced performance of the EWHE [9]. The effect of inlet temperature is shown in Figure 4.27, where inlet temperature was varied between 330 K and 350 K. The slope at an inlet temperature of 350 K is steeper compared to the other cases which indicates a greater heat exchange rate. Thus, inlet temperature is a significant parameter that has a major impact on the outcome of the heat exchanger [23]. The inlet temperature to the system will depend on the cooling load, a greater load results in a higher temperature.

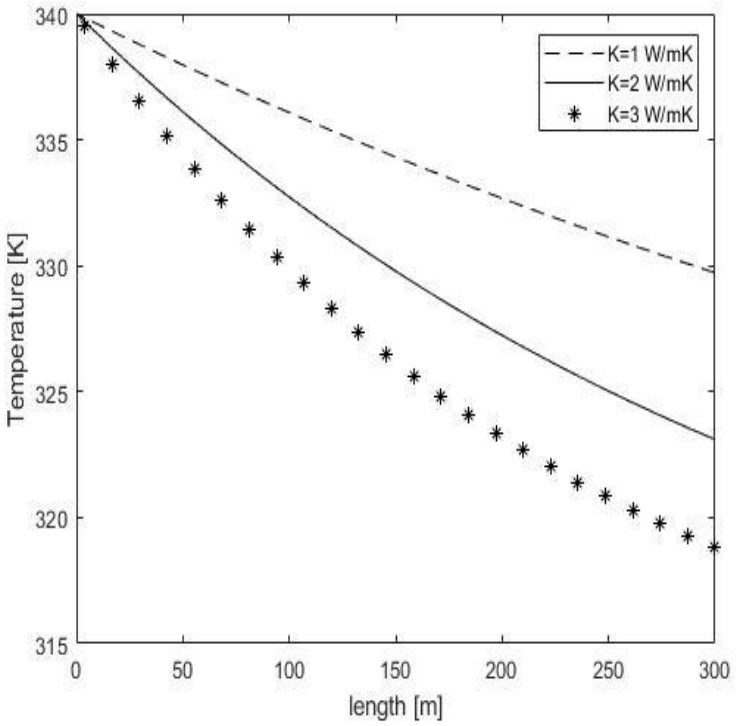

Figure 4.25: Effect of soil thermal conductivity on water outlet temperature.

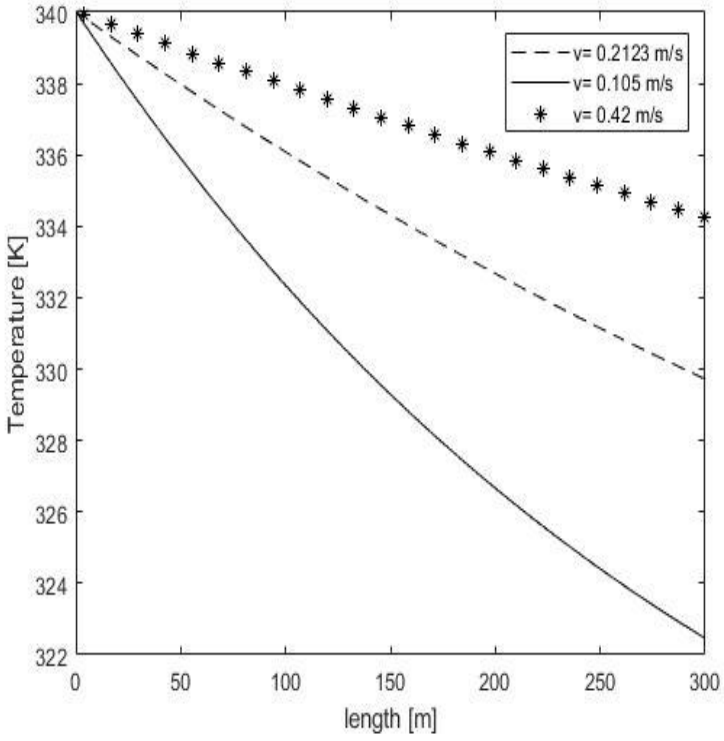

Figure 4.26: Effect of fluid velocity on water outlet temperature.

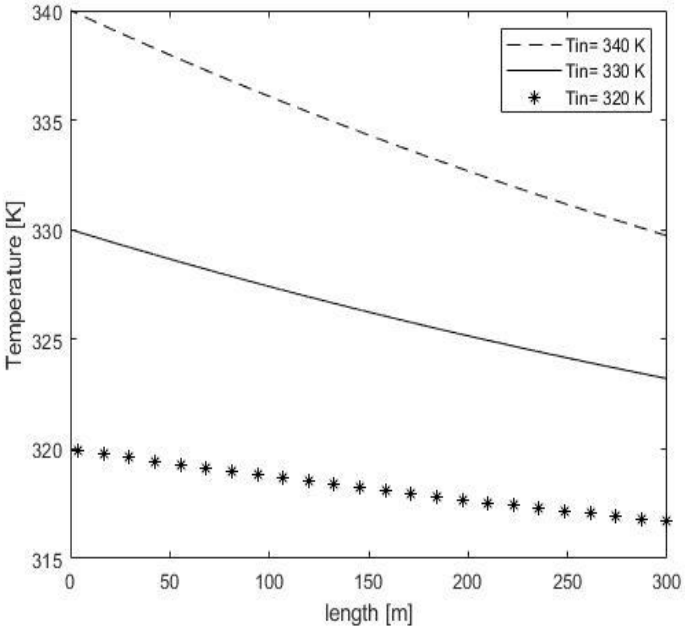

Figure 4.27: Effect of fluid inlet temperature on water outlet temperature.

Chapter 5. Conclusion and Future Work

This work determines the properties of soil and studies the performance of an Earth-Water heat exchanger based on data collected from the setup built at the University campus. Up-to-date work concludes the following:

1. The thermal conductivity of soil is significantly affected by water content and to a lesser extent influenced by the level of compaction with values ranging from 1 W/m.K to more than 2 W/m.K.
2. The temperature distribution predicted using Kasuda model is on average 3~4°C shifted from measured, overestimating the temperature in summer and underestimating in the winter.
3. There is a significant difference between ambient air temperature and the ground temperature at a depth of 2 meters suggesting a high geothermal cooling potential.
4. The ground temperature reaches a stable temperature at a depth of 8 m. This maybe assumed to be the ground undisturbed temperature and is equal to 32°C in contrast to 27°C predicted using Kasuda model.
5. The trench-setup provided a confirmation for the availability of a geothermal cooling potential in the UAE by achieving a decrease in outlet water temperature.
6. Higher inlet temperature results in a greater rate of heat exchange with a maximum of 19.1 kW.
7. Running the system continuously will reduce the effectiveness of the heat exchanger.

Overall, it can be concluded that the Earth Water Heat Exchanger is an effective method of cooling in the United Arab Emirates and can be further enhanced by adding backfill material. To facilitate the introduction of EWHEs, an economic feasibility study supported by an optimization criterion is required. Future studies may investigate the performance of a vertical EWHE using cement as backfield material in a borehole arrangement.

References

[1] J. Egg and B. C. Howard, *Geothermal HVAC*. McGraw-Hill Professional, 2010.

[2] M.-J. Kim, S.-R. Lee, S. Yoon, and G.-H. Go, "Thermal performance evaluation and parametric study of a horizontal ground heat exchanger," *Geothermics*, vol. 60, pp. 134–143, 2016.

[3] F. Niu, Y. Yu, D. Yu, and H. Li, "Heat and mass transfer performance analysis and cooling capacity prediction of earth to air heat exchanger," *Appl. Energy*, vol. 137, pp. 211–221, 2015.

[4] S. K. Soni, M. Pandey, and V. N. Bartaria, "Energy metrics of a hybrid earth air heat exchanger system for summer cooling requirements," *Energy Build.*, vol. 129, pp. 1–8, 2016.

[5] G. Hellström, B. Sanner, M. Klugescheid, T. Gonka, and S. Mårtensson, "Experiences with the borehole heat exchanger software EED," *Proc. Megastock*, vol. 97, pp. 247–252, 1997.

[6] A. Salem and H. Hashim, "A feasibility of geothermal cooling in Middle East," *Latest Trends Sustain. Green Dev*, pp. 105–112, 2010.

[7] A. Herez, M. Khaled, R. Murr, A. Haddad, H. Elhage, and M. Ramadan, "Using geothermal energy for cooling-parametric study," *Energy Procedia*, vol. 119, pp. 783–791, 2017.

[8] V. R. Tarnawski, W. H. Leong, T. Momose, and Y. Hamada, "Analysis of ground source heat pumps with horizontal ground heat exchangers for northern Japan," *Renew. Energy*, vol. 34, no. 1, pp. 127–134, 2009.

[9] M. H. Ali, K. Kariya, and A. Miyara, "Performance Analysis of Slinky Horizontal Ground Heat Exchangers for a Ground Source Heat Pump System," *Resources*, vol. 6, no. 4, p. 56, 2017.

[10] M. O. Hamdan, "Tapping to geothermal energy through a high performance earth-to-water heat exchanger design," in *2018 5th International Conference on Renewable Energy: Generation and Applications (ICREGA)*, 2018, pp. 207–210.

[11] J. Gao, A. Li, X. Xu, W. Gang, and T. Yan, "Ground heat exchangers: Applications, technology integration and potentials for zero energy buildings," *Renew. energy*, vol. 128, pp. 337–349, 2018.

[12] Z. Xiong, D. E. Fisher, and J. D. Spitler, "Development and validation of a Slinky^{TM} ground heat exchanger model," *Appl. Energy*, vol. 141, pp. 57–69, 2015.

[13] F. Ascione, D. D'Agostino, C. Marino, and F. Minichiello, "Earth-to-air heat exchanger for NZEB in Mediterranean climate," *Renew. energy*, vol. 99, pp. 553–563, 2016.

[14] S. Noor, W. Yang, M. Guo, K. H. van Dam, and X. Wang, "Energy Demand

Side Management within micro-grid networks enhanced by blockchain," *Appl. Energy*, vol. 228, pp. 1385–1398, 2018.

[15] S. K. Soni, M. Pandey, and V. N. Bartaria, "Ground coupled heat exchangers: A review and applications," *Renew. Sustain. Energy Rev.*, vol. 47, pp. 83–92, 2015.

[16] Y. Hwang *et al.*, "Cooling performance of a vertical ground-coupled heat pump system installed in a school building," *Renew. Energy*, vol. 34, no. 3, pp. 578–582, 2009.

[17] M. H. Sharqawy, S. A. Said, E. M. Mokheimer, M. A. Habib, H. M. Badr, and N. A. Al-Shayea, "First in situ determination of the ground thermal conductivity for boreholeheat exchanger applications in Saudi Arabia," *Renew. Energy*, vol. 34, no. 10, pp. 2218–2223, 2009.

[18] E. Pulat, S. Coskun, K. Unlu, and N. Yamankaradeniz, "Experimental study of horizontal ground source heat pump performance for mild climate in Turkey," *Energy*, vol. 34, no. 9, pp. 1284–1295, 2009.

[19] K. Bakirci, "Evaluation of the performance of a ground-source heat-pump system with series GHE (ground heat exchanger) in the cold climate region," *Energy*, vol. 35, no. 7, pp. 3088–3096, 2010.

[20] A. Miyara, K. Tsubaki, S. Inoue, and K. Yoshida, "Experimental study of several types of ground heat exchanger using a steel pile foundation," *Renew. Energy*, vol. 36, no. 2, pp. 764–771, 2011.

[21] G. A. Florides *et al.*, "The geothermal characteristics of the ground and the potential of using ground coupled heat pumps in Cyprus," *Energy*, vol. 36, no. 8, pp. 5027–5036, 2011.

[22] R. Karabacak, Ş. G. Acar, H. Kumsar, A. Gökgöz, M. Kaya, and Y. Tülek, "Experimental investigation of the cooling performance of a ground source heat pump system in Denizli, Turkey," *Int. J. Refrig.*, vol. 34, no. 2, pp. 454–465, 2011.

[23] N. Naili, M. Hazami, I. Attar, and A. Farhat, "In-field performance analysis of ground source cooling system with horizontal ground heat exchanger in Tunisia," *Energy*, vol. 61, pp. 319–331, 2013.

[24] A. Flaga-Maryanczyk, J. Schnotale, J. Radon, and K. Was, "Experimental measurements and CFD simulation of a ground source heat exchanger operating at a cold climate for a passive house ventilation system," *Energy Build.*, vol. 68, pp. 562–570, 2014.

[25] J. Vaz, M. A. Sattler, R. da S. Brum, E. D. dos Santos, and L. A. Isoldi, "An experimental study on the use of Earth-Air Heat Exchangers (EAHE)," *Energy Build.*, vol. 72, pp. 122–131, 2014.

[26] J. R. Cullin, F. Ruiz-Calvo, and P. E. JD Spitler PhD, "Experimental validation of ground heat exchanger design methodologies using real, monitored data," *ASHRAE Trans.*, vol. 120, p. 357, 2014.

[27] J. Luo, J. Rohn, M. Bayer, A. Priess, L. Wilkmann, and W. Xiang, "Heating

and cooling performance analysis of a ground source heat pump system in Southern Germany," *Geothermics*, vol. 53, pp. 57–66, 2015.

[28] A. A. Serageldin, A. K. Abdelrahman, and S. Ookawara, "Earth-Air Heat Exchanger thermal performance in Egyptian conditions: Experimental results, mathematical model, and Computational Fluid Dynamics simulation," *Energy Convers. Manag.*, vol. 122, pp. 25–38, 2016.

[29] T. Sivasakthivel, K. Murugesan, S. Kumar, P. Hu, and P. Kobiga, "Experimental study of thermal performance of a ground source heat pump system installed in a Himalayan city of India for composite climatic conditions," *Energy Build.*, vol. 131, pp. 193–206, 2016.

[30] T. Sivasakthivel, M. Philippe, K. Murugesan, V. Verma, and P. Hu, "Experimental thermal performance analysis of ground heat exchangers for space heating and cooling applications," *Renew. Energy*, vol. 113, pp. 1168–1181, 2017.

[31] X. Q. Zhai, X. W. Cheng, and R. Z. Wang, "Heating and cooling performance of a minitype ground source heat pump system," *Appl. Therm. Eng.*, vol. 111, pp. 1366–1370, 2017.

[32] Y. Man, H. Yang, N. Diao, J. Liu, and Z. Fang, "A new model and analytical solutions for borehole and pile ground heat exchangers," *Int. J. Heat Mass Transf.*, vol. 53, no. 13–14, pp. 2593–2601, 2010.

[33] N. Molina-Giraldo, P. Blum, K. Zhu, P. Bayer, and Z. Fang, "A moving finite line source model to simulate borehole heat exchangers with groundwater advection," *Int. J. Therm. Sci.*, vol. 50, no. 12, pp. 2506–2513, 2011.

[34] G. Florides *et al.*, "Modeling and assessment of the efficiency of horizontal and vertical ground heat exchangers," *Energy*, vol. 58, pp. 655–663, 2013.

[35] T. S. Bisoniya, "Design of earth–air heat exchanger system," *Geotherm. Energy*, vol. 3, no. 1, p. 18, 2015.

[36] K. Kupiec, B. Larwa, and M. Gwadera, "Heat transfer in horizontal ground heat exchangers," *Appl. Therm. Eng.*, vol. 75, pp. 270–276, 2015.

[37] H. Demir, A. Koyun, and G. Temir, "Heat transfer of horizontal parallel pipe ground heat exchanger and experimental verification," *Appl. Therm. Eng.*, vol. 29, no. 2–3, pp. 224–233, 2009.

[38] Z. Li and M. Zheng, "Development of a numerical model for the simulation of vertical U-tube ground heat exchangers," *Appl. Therm. Eng.*, vol. 29, no. 5–6, pp. 920–924, 2009.

[39] Y. Wu, G. Gan, A. Verhoef, P. L. Vidale, and R. G. Gonzalez, "Experimental measurement and numerical simulation of horizontal-coupled slinky ground source heat exchangers," *Appl. Therm. Eng.*, vol. 30, no. 16, pp. 2574–2583, 2010.

[40] V. Bansal, R. Misra, G. Das Agrawal, and J. Mathur, "Performance analysis of earth–pipe–air heat exchanger for summer cooling," *Energy Build.*, vol. 42, no. 5, pp. 645–648, 2010.

[41] Y. Shang, S. Li, and H. Li, “Analysis of geo-temperature recovery under intermittent operation of ground-source heat pump,” *Energy Build.*, vol. 43, no. 4, pp. 935–943, 2011.

[42] A. Benazza, E. Blanco, M. Aichouba, J. L. Río, and S. Laouedj, “Numerical investigation of horizontal ground coupled heat exchanger,” *Energy Procedia*, vol. 6, pp. 29–35, 2011.

[43] V. Khalajzadeh, G. Heidarinejad, and J. Srebric, “Parameters optimization of a vertical ground heat exchanger based on response surface methodology,” *Energy Build.*, vol. 43, no. 6, pp. 1288–1294, 2011.

[44] P. M. Congedo, G. Colangelo, and G. Starace, “CFD simulations of horizontal ground heat exchangers: A comparison among different configurations,” *Appl. Therm. Eng.*, vol. 33, pp. 24–32, 2012.

[45] H. Fujii, K. Nishi, Y. Komaniwa, and N. Chou, “Numerical modeling of slinky-coil horizontal ground heat exchangers,” *Geothermics*, vol. 41, pp. 55–62, 2012.

[46] C. S. A. Chong, G. Gan, A. Verhoef, R. G. Garcia, and P. L. Vidale, “Simulation of thermal performance of horizontal slinky-loop heat exchangers for ground source heat pumps,” *Appl. Energy*, vol. 104, pp. 603–610, 2013.

[47] R. Misra, V. Bansal, G. Das Agrawal, J. Mathur, and T. K. Aseri, “CFD analysis based parametric study of derating factor for Earth Air Tunnel Heat Exchanger,” *Appl. Energy*, vol. 103, pp. 266–277, 2013.

[48] T. S. Bisoniya, A. Kumar, and P. Baredar, “Energy metrics of earth–air heat exchanger system for hot and dry climatic conditions of India,” *Energy Build.*, vol. 86, pp. 214–221, 2015.

[49] M. Bottarelli, M. Bortoloni, Y. Su, C. Yousif, A. A. Aydın, and A. Georgiev, “Numerical analysis of a novel ground heat exchanger coupled with phase change materials,” *Appl. Therm. Eng.*, vol. 88, pp. 369–375, 2015.

[50] A. Bidarmaghz, G. A. Narsilio, I. W. Johnston, and S. Colls, “The importance of surface air temperature fluctuations on long-term performance of vertical ground heat exchangers,” *Geomech. Energy Environ.*, vol. 6, pp. 35–44, 2016.

[51] P. Congedo, C. Lorusso, M. De Giorgi, R. Marti, and D. D’Agostino, “Horizontal air-ground heat exchanger performance and humidity simulation by computational fluid dynamic analysis,” *Energies*, vol. 9, no. 11, p. 930, 2016.

[52] M. Bortoloni, M. Bottarelli, and Y. Su, “A study on the effect of ground surface boundary conditions in modelling shallow ground heat exchangers,” *Appl. Therm. Eng.*, vol. 111, pp. 1371–1377, 2017.

[53] R. Sangi and D. Müller, “Dynamic modelling and simulation of a slinky-coil horizontal ground heat exchanger using Modelica,” *J. Build. Eng.*, vol. 16, pp. 159–168, 2018.

[54] A. Zarrella, M. De Carli, and A. Galgaro, “Thermal performance of two types of energy foundation pile: helical pipe and triple U-tube,” *Appl. Therm. Eng.*,

vol. 61, no. 2, pp. 301–310, 2013.

[55] S. Park, C. Sung, K. Jung, B. Sohn, A. Chauchois, and H. Choi, "Constructability and heat exchange efficiency of large diameter cast-in-place energy piles with various configurations of heat exchange pipe," *Appl. Therm. Eng.*, vol. 90, pp. 1061–1071, 2015.

[56] Q. Zhao, B. Chen, and F. Liu, "Study on the thermal performance of several types of energy pile ground heat exchangers: U-shaped, W-shaped and spiral-shaped," *Energy Build.*, vol. 133, pp. 335–344, 2016.

[57] B. Dehghan, "Effectiveness of using spiral ground heat exchangers in ground source heat pump system of a building for district heating/cooling purposes: Comparison among different configurations," *Appl. Therm. Eng.*, vol. 130, pp. 1489–1506, 2018.

[58] D. Quaggiotto *et al.*, "Simulation-Based Comparison Between the Thermal Behavior of Coaxial and Double U-Tube Borehole Heat Exchangers," *Energies*, vol. 12, no. 12, p. 2321, 2019.

[59] H. Javadi, S. S. M. Ajarostaghi, M. Pourfallah, and M. Zaboli, "Performance analysis of helical ground heat exchangers with different configurations," *Appl. Therm. Eng.*, vol. 154, pp. 24–36, 2019.

[60] S. Yoon, S.-R. Lee, and G.-H. Go, "Evaluation of thermal efficiency in different types of horizontal ground heat exchangers," *Energy Build.*, vol. 105, pp. 100–105, 2015.

[61] S. Selamat, A. Miyara, and K. Kariya, "Numerical study of horizontal ground heat exchangers for design optimization," *Renew. energy*, vol. 95, pp. 561–573, 2016.

[62] M. Habibi and A. Hakkaki-Fard, "Evaluation and improvement of the thermal performance of different types of horizontal ground heat exchangers based on techno-economic analysis," *Energy Convers. Manag.*, vol. 171, pp. 1177–1192, 2018.

[63] A. Zarrella and M. De Carli, "Heat transfer analysis of short helical borehole heat exchangers," *Appl. Energy*, vol. 102, pp. 1477–1491, 2013.

[64] F. Robert and L. Gosselin, "New methodology to design ground coupled heat pump systems based on total cost minimization," *Appl. Therm. Eng.*, vol. 62, no. 2, pp. 481–491, 2014.

[65] L. Pu, D. Qi, K. Li, H. Tan, and Y. Li, "Simulation study on the thermal performance of vertical U-tube heat exchangers for ground source heat pump system," *Appl. Therm. Eng.*, vol. 79, pp. 202–213, 2015.

[66] R. R. Dasare and S. K. Saha, "Numerical study of horizontal ground heat exchanger for high energy demand applications," *Appl. Therm. Eng.*, vol. 85, pp. 252–263, 2015.

[67] B. Dehghan, A. Sisman, and M. Aydin, "Parametric investigation of helical ground heat exchangers for heat pump applications," *Energy Build.*, vol. 127, pp. 999–1007, 2016.

[68] N. Kayaci and H. Demir, “Numerical modelling of transient soil temperature distribution for horizontal ground heat exchanger of ground source heat pump,” *Geothermics*, vol. 73, pp. 33–47, 2018.

[69] A. Zarrella, G. Emmi, and M. De Carli, “Analysis of operating modes of a ground source heat pump with short helical heat exchangers,” *Energy Convers. Manag.*, vol. 97, pp. 351–361, 2015.

[70] L. Pu, L. Xu, D. Qi, and Y. Li, “Structure optimization for horizontal ground heat exchanger,” *Appl. Therm. Eng.*, vol. 136, pp. 131–140, 2018.

[71] Y. Wu, G. Gan, R. G. Gonzalez, A. Verhoef, and P. L. Vidale, “Prediction of the thermal performance of horizontal-coupled ground-source heat exchangers,” *Int. J. Low-Carbon Technol.*, vol. 6, no. 4, pp. 261–269, 2011.

[72] F. Droulia, S. Lykoudis, I. Tsiros, N. Alvertos, E. Akylas, and I. Garofalakis, “Ground temperature estimations using simplified analytical and semi-empirical approaches,” *Sol. Energy*, vol. 83, no. 2, pp. 211–219, 2009.

[73] O. Ozgener, L. Ozgener, and J. W. Tester, “A practical approach to predict soil temperature variations for geothermal (ground) heat exchangers applications,” *Int. J. Heat Mass Transf.*, vol. 62, pp. 473–480, 2013.

[74] C. O. Popiel and J. Wojtkowiak, “Temperature distributions of ground in the urban region of Poznan City,” *Exp. Therm. Fluid Sci.*, vol. 51, pp. 135–148, 2013.

[75] G. Tsilingiridis and K. Papakostas, “Investigating the relationship between air and ground temperature variations in shallow depths in northern Greece,” *Energy*, vol. 73, pp. 1007–1016, 2014.

[76] H. Xu and J. D. Spitler, “The relative importance of moisture transfer, soil freezing and snow cover on ground temperature predictions,” *Renew. energy*, vol. 72, pp. 1–11, 2014.

[77] M. Ouzzane, P. Eslami-Nejad, M. Badache, and Z. Aidoun, “New correlations for the prediction of the undisturbed ground temperature,” *Geothermics*, vol. 53, pp. 379–384, 2015.

[78] V. Soldo, L. Boban, and S. Borović, “Vertical distribution of shallow ground thermal properties in different geological settings in Croatia,” *Renew. energy*, vol. 99, pp. 1202–1212, 2016.

[79] M. Badache, P. Eslami-Nejad, M. Ouzzane, Z. Aidoun, and L. Lamarche, “A new modeling approach for improved ground temperature profile determination,” *Renew. Energy*, vol. 85, pp. 436–444, 2016.

[80] I. V Nikolaev, W. H. Leong, and M. A. Rosen, “Experimental investigation of soil thermal conductivity over a wide temperature range,” *Int. J. Thermophys.*, vol. 34, no. 6, pp. 1110–1129, 2013.

[81] D. Barry-Macaulay, A. Bouazza, R. M. Singh, B. Wang, and P. G. Ranjith, “Thermal conductivity of soils and rocks from the Melbourne (Australia) region,” *Eng. Geol.*, vol. 164, pp. 131–138, 2013.

[82] N. Lu and Y. Dong, “Closed-form equation for thermal conductivity of unsaturated soils at room temperature,” *J. Geotech. Geoenvironmental Eng.*, vol. 141, no. 6, p. 4015016, 2015.

[83] F. Gori and S. Corasaniti, “New model to evaluate the effective thermal conductivity of three-phase soils,” *Int. Commun. Heat Mass Transf.*, vol. 47, pp. 1–6, 2013.

[84] A. Alrtimi, M. Rouainia, and S. Haigh, “Thermal conductivity of a sandy soil,” *Appl. Therm. Eng.*, vol. 106, pp. 551–560, 2016.

[85] D. A. De Vries, “Thermal properties of soils,” *Phys. plant Environ.*, 1963.

[86] J. Côté and J.-M. Konrad, “A generalized thermal conductivity model for soils and construction materials,” *Can. Geotech. J.*, vol. 42, no. 2, pp. 443–458, 2005.

[87] S. Lu, T. Ren, Y. Gong, and R. Horton, “An improved model for predicting soil thermal conductivity from water content at room temperature,” *Soil Sci. Soc. Am. J.*, vol. 71, no. 1, pp. 8–14, 2007.

[88] S. K. Haigh, “Thermal conductivity of sands,” *Geotechnique*, vol. 62, no. 7, p. 617, 2012.

[89] Y. Man, H. Yang, and J. Wang, “Study on hybrid ground-coupled heat pump system for air-conditioning in hot-weather areas like Hong Kong,” *Appl. Energy*, vol. 87, no. 9, pp. 2826–2833, 2010.

[90] X. Wang, M. Zheng, W. Zhang, S. Zhang, and T. Yang, “Experimental study of a solar-assisted ground-coupled heat pump system with solar seasonal thermal storage in severe cold areas,” *Energy Build.*, vol. 42, no. 11, pp. 2104–2110, 2010.

[91] C. Xi, L. Lin, and Y. Hongxing, “Long term operation of a solar assisted ground coupled heat pump system for space heating and domestic hot water,” *Energy Build.*, vol. 43, no. 8, pp. 1835–1844, 2011.

[92] C. Xi, Y. Hongxing, L. Lin, W. Jinggang, and L. Wei, “Experimental studies on a ground coupled heat pump with solar thermal collectors for space heating,” *Energy*, vol. 36, no. 8, pp. 5292–5300, 2011.

[93] Y. Man, H. Yang, J. D. Spitler, and Z. Fang, “Feasibility study on novel hybrid ground coupled heat pump system with nocturnal cooling radiator for cooling load dominated buildings,” *Appl. Energy*, vol. 88, no. 11, pp. 4160–4171, 2011.

[94] E. Wang, A. S. Fung, C. Qi, and W. H. Leong, “Build-up and long-term performance prediction of a hybrid solar ground source heat pump system for office building in cold climate,” *Proc. eSim*, 2012.

[95] F. M. Rad, A. S. Fung, and W. H. Leong, “Feasibility of combined solar thermal and ground source heat pump systems in cold climate, Canada,” *Energy Build.*, vol. 61, pp. 224–232, 2013.

[96] R. Fan, Y. Gao, L. Hua, X. Deng, and J. Shi, “Thermal performance and operation strategy optimization for a practical hybrid ground-source heat-pump

system," *Energy Build.*, vol. 78, pp. 238–247, 2014.

[97] J. Yang, L. Xu, P. Hu, N. Zhu, and X. Chen, "Study on intermittent operation strategies of a hybrid ground-source heat pump system with double-cooling towers for hotel buildings," *Energy Build.*, vol. 76, pp. 506–512, 2014.

[98] L. Dai, S. Li, L. DuanMu, X. Li, Y. Shang, and M. Dong, "Experimental performance analysis of a solar assisted ground source heat pump system under different heating operation modes," *Appl. Therm. Eng.*, vol. 75, pp. 325–333, 2015.

[99] A. Chel and G. N. Tiwari, "Stand-alone photovoltaic (PV) integrated with earth to air heat exchanger (EAHE) for space heating/cooling of adobe house in New Delhi (India)," *Energy Convers. Manag.*, vol. 51, no. 3, pp. 393–409, 2010.

[100] M. Maerefat and A. P. Haghighi, "Passive cooling of buildings by using integrated earth to air heat exchanger and solar chimney," *Renew. Energy*, vol. 35, no. 10, pp. 2316–2324, 2010.

[101] S. Jakhar, R. Misra, M. S. Soni, and N. Gakkhar, "Parametric simulation and experimental analysis of earth air heat exchanger with solar air heating duct," *Eng. Sci. Technol. an Int. J.*, vol. 19, no. 2, pp. 1059–1066, 2016.

[102] S. Awani, S. Kooli, R. Chargui, and A. Guizani, "Numerical and experimental study of a closed loop for ground heat exchanger coupled with heat pump system and a solar collector for heating a glass greenhouse in north of Tunisia," *Int. J. Refrig.*, vol. 76, pp. 328–341, 2017.

[103] C. D. Argyropoulos and N. C. Markatos, "Recent advances on the numerical modelling of turbulent flows," *Appl. Math. Model.*, vol. 39, no. 2, pp. 693–732, 2015.

[104] C. O. Popiel, J. Wojtkowiak, and B. Biernacka, "Measurements of temperature distribution in ground," *Exp. Therm. fluid Sci.*, vol. 25, no. 5, pp. 301–309, 2001.

[105] T. Kusuda and P. R. Achenbach, "Earth temperature and thermal diffusivity at selected stations in the United States," National Bureau of Standards Gaithersburg MD, 1965.

[106] B. Tong, Z. Gao, R. Horton, Y. Li, and L. Wang, "An empirical model for estimating soil thermal conductivity from soil water content and porosity," *J. Hydrometeorol.*, vol. 17, no. 2, pp. 601–613, 2016.

Vita

Hanin Atwany was born in 1996 in Amman, Jordan. She received her primary and secondary education in Al-Ansar School, Sharjah, UAE. She continued her post-secondary education and obtained a B.Sc. degree in Sustainable and Renewable Energy Engineering from the University of Sharjah in December 2017

In January 2018, she joined the Mechanical Engineering master's program at the American University of Sharjah as a graduate teaching assistant. During her master's study, she co-authored two journal papers in addition to two conference papers, which were presented in international conferences.